

12-9-2011

# Wnt signaling exerts an antiproliferative effect on adult cardiac progenitor cells through IGFBP3.

Angelos Oikonomopoulos

*Cardiac Muscle Research Laboratory; University of Crete*

Konstantina-Ioanna Sereti

*Cardiac Muscle Research Laboratory; University of Crete*

Frank Conyers

*Cardiac Muscle Research Laboratory*


Michael Bauer

*Cardiac Muscle Research Laboratory*

Annette Liao

*Cardiac Muscle Research Laboratory**See next page for additional authors*

## [Let us know how access to this document benefits you](#)

Follow this and additional works at: <http://jdc.jefferson.edu/transmedfp> Part of the [Cardiology Commons](#), and the [Medical Cell Biology Commons](#)

### Recommended Citation

Oikonomopoulos, Angelos; Sereti, Konstantina-Ioanna; Conyers, Frank; Bauer, Michael; Liao, Annette; Guan, Jian; Crapps, Dylan; Han, Jung-Kyu; Dong, Hanhua; Bayomy, Ahmad F; Fine, Gabriel C; Westerman, Karen; Biechele, Travis L; Moon, Randall T; Force, Thomas; and Liao, Ronglih, "Wnt signaling exerts an antiproliferative effect on adult cardiac progenitor cells through IGFBP3." (2011). *Center for Translational Medicine Faculty Papers*. Paper 9.  
<http://jdc.jefferson.edu/transmedfp/9>

---

**Authors**

Angelos Oikonomopoulos, Konstantina-Ioanna Sereti, Frank Conyers, Michael Bauer, Annette Liao, Jian Guan, Dylan Crapps, Jung-Kyu Han, Hanhua Dong, Ahmad F Bayomy, Gabriel C Fine, Karen Westerman, Travis L Biechele, Randall T Moon, Thomas Force, and Ronglih Liao

## Wnt Signaling Exerts an Antiproliferative Effect on Adult Cardiac Progenitor Cells Through IGFBP3

Angelos Oikonomopoulos, Konstantina-Ioanna Sereti, Frank Conyers, Michael Bauer, Annette Liao, Jian Guan, Dylan Crapps, Jung-Kyu Han, Hanhua Dong, Ahmad F. Bayomy, Gabriel C. Fine, Karen Westerman, Travis L. Biechele, Randall T. Moon, Thomas Force and Ronglih Liao

*Circ Res.* 2011;109:1363-1374; originally published online October 27, 2011;  
doi: 10.1161/CIRCRESAHA.111.250282

*Circulation Research* is published by the American Heart Association, 7272 Greenville Avenue, Dallas, TX 75231  
Copyright © 2011 American Heart Association, Inc. All rights reserved.  
Print ISSN: 0009-7330. Online ISSN: 1524-4571

The online version of this article, along with updated information and services, is located on the  
World Wide Web at:

<http://circres.ahajournals.org/content/109/12/1363>

Data Supplement (unedited) at:

<http://circres.ahajournals.org/content/suppl/2011/10/27/CIRCRESAHA.111.250282.DC1.html>

**Permissions:** Requests for permissions to reproduce figures, tables, or portions of articles originally published in *Circulation Research* can be obtained via RightsLink, a service of the Copyright Clearance Center, not the Editorial Office. Once the online version of the published article for which permission is being requested is located, click Request Permissions in the middle column of the Web page under Services. Further information about this process is available in the [Permissions and Rights Question and Answer](#) document.

**Reprints:** Information about reprints can be found online at:  
<http://www.lww.com/reprints>

**Subscriptions:** Information about subscribing to *Circulation Research* is online at:  
<http://circres.ahajournals.org/subscriptions/>

## Wnt Signaling Exerts an Antiproliferative Effect on Adult Cardiac Progenitor Cells Through IGFBP3

Angelos Oikonomopoulos, Konstantina-Ioanna Sereti, Frank Conyers, Michael Bauer, Annette Liao, Jian Guan, Dylan Crapps, Jung-Kyu Han, Hanhua Dong, Ahmad F. Bayomy, Gabriel C. Fine, Karen Westerman, Travis L. Biechele, Randall T. Moon, Thomas Force, Ronglih Liao

**Rationale:** Recent work in animal models and humans has demonstrated the presence of organ-specific progenitor cells required for the regenerative capacity of the adult heart. In response to tissue injury, progenitor cells differentiate into specialized cells, while their numbers are maintained through mechanisms of self-renewal. The molecular cues that dictate the self-renewal of adult progenitor cells in the heart, however, remain unclear.

**Objective:** We investigate the role of canonical Wnt signaling on adult cardiac side population (CSP) cells under physiological and disease conditions.

**Methods and Results:** CSP cells isolated from C57BL/6J mice were used to study the effects of canonical Wnt signaling on their proliferative capacity. The proliferative capacity of CSP cells was also tested after injection of recombinant Wnt3a protein (r-Wnt3a) in the left ventricular free wall. Wnt signaling was found to decrease the proliferation of adult CSP cells, both in vitro and in vivo, through suppression of cell cycle progression. Wnt stimulation exerted its antiproliferative effects through a previously unappreciated activation of insulin-like growth factor binding protein 3 (IGFBP3), which requires intact IGF binding site for its action. Moreover, injection of r-Wnt3a after myocardial infarction in mice showed that Wnt signaling limits CSP cell renewal, blocks endogenous cardiac regeneration and impairs cardiac performance, highlighting the importance of progenitor cells in maintaining tissue function after injury.

**Conclusions:** Our study identifies canonical Wnt signaling and the novel downstream mediator, IGFBP3, as key regulators of adult cardiac progenitor self-renewal in physiological and pathological states. (*Circ Res.* 2011;109:1363-1374.)

**Key Words:** cardiac side population cells ■ Wnt signaling ■ cardiac regeneration ■ stem cells ■ proliferation

Accumulating evidence over the past decade in both humans and animal models has documented the presence of endogenous progenitor cells in adult myocardium.<sup>1-6</sup> In response to local tissue injury, cardiac progenitor cells differentiate into specialized cells, while the pool of progenitor cells is maintained, in part, through self-renewal and enhanced proliferation.<sup>7,8</sup> However, the molecular cues and signaling pathways that dictate the homeostasis of adult progenitor cells and in particular their self-renewal, in physiological and pathological states, remain unclear.

Wnt ligands constitute a family of 19 secreted glycoproteins that act as key regulators of cellular function during

development, adulthood, and disease.<sup>9,10</sup> Several reports have proposed time and context dependent roles for Wnt signaling in cardiogenesis and progenitor cell biology.<sup>11</sup> Studies in chick and *Xenopus* embryos have demonstrated that inhibition of Wnt signaling is required for cardiac differentiation,<sup>12,13</sup> whereas Wnt signaling has also been found to promote cardiomyogenesis in *Drosophila* and embryonic carcinoma P19 cells.<sup>14,15</sup> Moreover, early in gastrulation, Wnt ligands activate a cardiac differentiation program, whereas at later stages they act as potent inhibitors of the cardiomyogenic differentiation.<sup>16,17</sup> Recent genetic studies have demonstrated that the canonical Wnt signaling cascade promotes the

Original received June 15, 2011; revision received October 14, 2011; accepted October 20, 2011. In September 2011, the average time from submission to first decision for all original research papers submitted to *Circulation Research* was 16 days.

From the Cardiovascular Division, the Department of Medicine, Brigham and Women's Hospital, Harvard Medical School, Boston, MA (A.O., K.-I.S., F.C., M.B., A.L., J.G., D.C., J.-K.H., H.D., A.F.B., G.C.F., R.L.); University of Crete Medical School, Heraklion, Greece (A.O., K.-I.S.); Hepatic Surgery Centre, Tongji Hospital, and Huazhong University of Science and Technology, Wuhan, China (H.D.); University of Washington School of Medicine, Seattle, WA (A.F.B., G.C.F.); the Department of Anesthesia, Perioperative and Pain Medicine, Brigham and Women's Hospital, Boston, MA (K.W.); Howard Hughes Medical Institute, the Department of Pharmacology, and Institute for Stem Cell and Regenerative Medicine, University of Washington School of Medicine, Seattle, WA (T.L.B., R.T.M.); and the Center for Translational Medicine and the Cardiology Division, Thomas Jefferson University Hospital, Philadelphia, PA (T.F.).

Correspondence to Ronglih Liao, PhD, Cardiac Muscle Research Laboratory, Cardiovascular Division, Department of Medicine, Brigham and Women's Hospital, Harvard Medical School, 77 Avenue Louis Pasteur, NRB 431, Boston, MA 02115. E-mail rliao@rics.bwh.harvard.edu

© 2011 American Heart Association, Inc.

*Circulation Research* is available at <http://circres.ahajournals.org>

DOI: 10.1161/CIRCRESAHA.111.250282

**Non-standard Abbreviations and Acronyms**

<b>CSP</b>	cardiac side population
<b>IGF</b>	insulin growth factor
<b>IGFBP3</b>	insulin growth factor binding protein 3
<b>MI</b>	myocardial infarction
<b>SP</b>	side population

proliferation of neonatal and embryonic Isl-1<sup>+</sup> cardiac progenitors in vitro and in vivo.<sup>18–20</sup> Little is known, however, regarding the role of Wnt signals in modulating adult progenitor cell populations.

Side population (SP) cells were initially identified based on their unique ability to efflux the DNA binding dye Hoechst 33342,<sup>21</sup> and were found to retain the long-term regenerative potential of bone marrow. Subsequently, SP cells were identified in various adult tissues/organs including adult myocardium.<sup>22</sup> Cardiac SP (CSP) cells are enriched in Scal but do not express c-kit or Isl-1.<sup>6</sup> More importantly, CSP cells are found to be capable of differentiation into functional cardiac myocytes in vitro or in vivo after myocardial infarction (MI).<sup>6,23–25</sup> We demonstrate that in contrast to previous work in embryonic or early postnatal stem cells, Wnt signaling negatively regulates the proliferation of adult CSP progenitor cells, both in vitro and in vivo, through suppression of cell cycle progression. Moreover, Wnt activation exerts its antiproliferative effects through a previously unappreciated activation of IGFBP3, which is found to require intact IGF binding site for its action. Importantly, activation of Wnt signaling was found to limit CSP cell renewal after MI, impair endogenous regenerative capacity, and worsen post-MI structural and functional remodeling. Overall, our study represents the first investigation of the role of canonical Wnt pathway in the homeostasis of adult cardiac progenitor cells in both physiological and pathological states and highlights the importance of cardiac progenitor cells in maintaining tissue function after injury.

## Methods

An expanded Methods section describing all procedures and protocols is available in the Online Data Supplement at <http://circres.ahajournals.org>.

## Animals

C57BL/6J male and female mice (8–12 weeks old) were purchased from Jackson Laboratory (Jackson East, MP 15). All animal procedures and handling were performed under the guidelines of Harvard Medical School, the Longwood Medical Area Institutional Animal Care and Use Committee (IACUC), and the National Society for Medical Research. MI was generated in C57BL/6J female mice as previously described.<sup>26</sup> MI size was estimated using histological imaging of three transverse myocardial sections (base, midpapillary, and apex) after staining with Masson trichrome, as previously described.<sup>27</sup>

## Intramyocardial Injection of Recombinant Wnt3a or Recombinant IGFBP3

Ten microliters of recombinant Wnt3a (r-Wnt3a, 400 ng) or recombinant IGFBP3 (r-IGFBP3) proteins (1000 ng) (R&D) or vehicle

(PBS) was given by intramyocardial injection into 3 sites of the left ventricular free wall of nonsurgically operated female mice (r-Wnt3a) or into the infarct/border zone area of mice immediately after MI (r-Wnt3a or r-IGFBP3).

## Heart Fixation and Histology

One day after echocardiographic measurements, animals were euthanized and hearts were fixed at an end-diastolic pressure of 5 mm Hg, using a Langendorff apparatus. For details, see Methods in the Online Data Supplement.

## Echocardiography

Echocardiography was performed 1 day before MI and 7 days after MI using a high-resolution, high-frequency digital imaging system (Vevo 2100, VisualSonics), as previously described.<sup>28</sup> For details, see Methods in the Online Data Supplement.

## FACS Analysis

FACS was performed using a FACSAria (Becton Dickinson, BD) equipped with 3 lasers (488 nm, 633 nm, 355 nm). Hoechst 33342 dye was excited by an UV (355 nm) laser. Acquired data were analyzed by FACSDIVA software (BD Biosciences).

## RNA Isolation and RT-PCR

RNA was extracted from CSP cells using Trizol reagent (Invitrogen) followed by RNeasy Mini Kit (Qiagen). Genomic DNA was removed using Turbo-DNA free kit (Ambion). cDNA was generated using a reverse transcription synthesis kit (Bio-Rad) and RT-PCR was performed in a MyiQ cycler (Bio-Rad). Primer sequences are available on request.

## Luciferase Assays

Luciferase activity was measured using a dual luciferase kit (Promega). Cell lysates were prepared from trypsinized CSP cells and used to determine the values of *Firefly* and *Renilla* luciferases, with a 20/20<sup>n</sup> Luminometer (Turner Biosystems).

## Statistical Analysis

Statistical differences were evaluated using 1-way ANOVA analysis and Student unpaired *t* test, using GraphPad Prism (Version 5.03). Data are presented as mean ± SEM. A probability value ≤ 0.05 was considered statistically significant.

## Results

### Wnt3a Negatively Regulates the Growth Potential of CSP Cells Both In Vitro and In Vivo

Given the context dependency of Wnt signaling, we examined the role of Wnt signals in mediating the proliferative capacity of adult CSP cells. Under unstimulated conditions, application of recombinant SFRP2 (Soluble Frizzled-related Protein 2), a known Wnt antagonist,<sup>29</sup> did not affect the proliferation capacity of CSP cells in vitro, suggesting that Wnt activity in baseline CSP cells in vitro is relatively low (Online Figure I). Treatment of CSP cells with increasing doses of Wnt3a-conditioned medium (Wnt3a-CM) resulted in a gradual activation of the canonical Wnt signaling pathway, as assessed by a T-cell factor-controlled luciferase reporter assay<sup>30</sup> and a respective decrease in CSP cell number, in comparison to vehicle-conditioned medium treated cells (Figure 1A and 1B). A similar decrease in cell proliferation in response to activation of canonical Wnt signaling was also observed in CSP cells treated with recombinant Wnt3a protein (r-Wnt3a) (Figure 1C and 1D). Likewise, BIO ((2'Z, 3'E)-6-

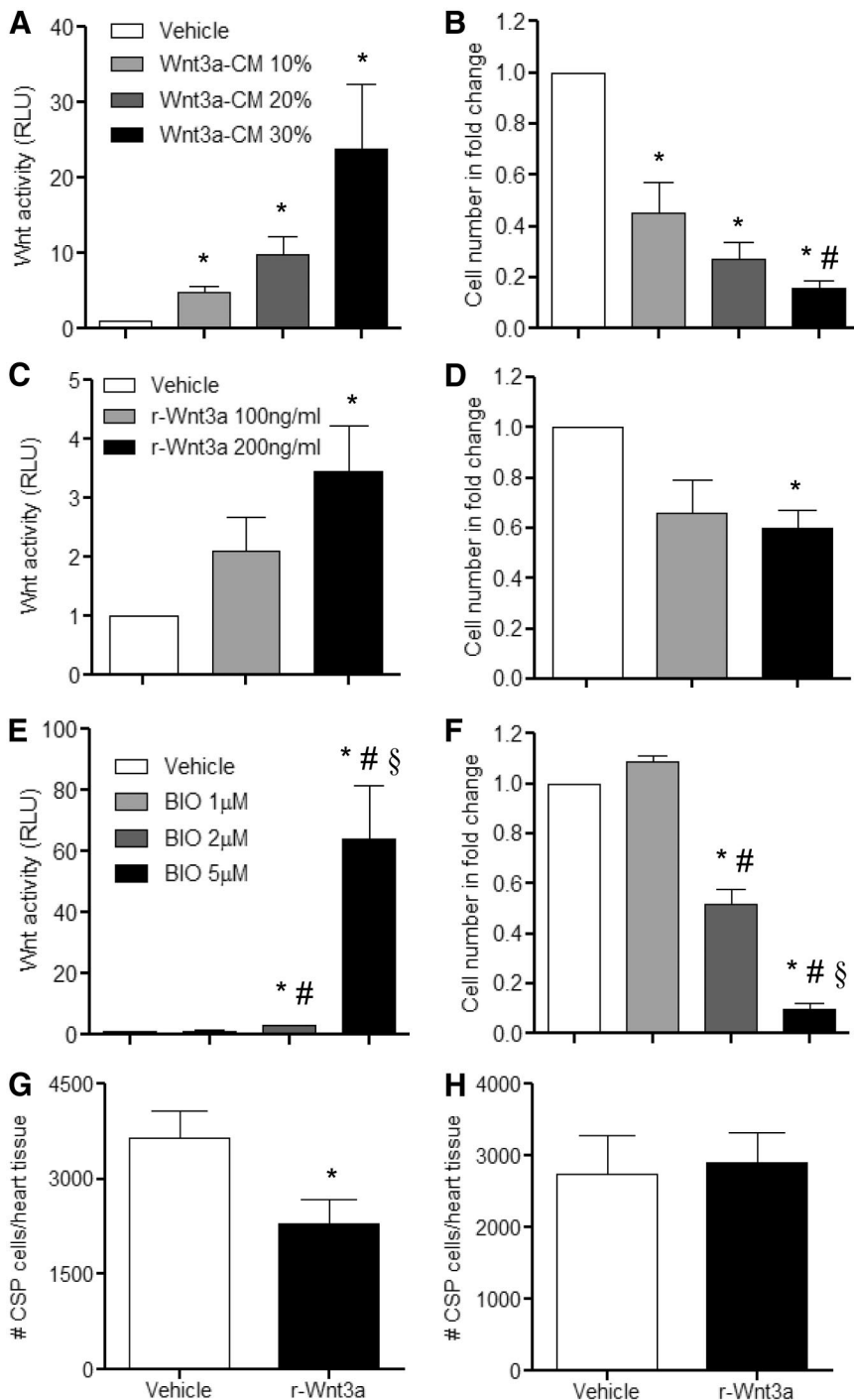


**Figure 1. Canonical Wnt signaling pathway mediates antigrowth effects on CSP cells.** Treatment of CSP cells with increasing concentrations of **A**, Wnt3a-CM (n=3); **C**, r-Wnt3a (n=3); and **E**, BIO (n=6) activated the canonical Wnt signaling pathway, as measured by the T-cell factor–luciferase reporter assay. Corresponding proliferation assays using the same dosages of **B**, Wnt3a-CM (n=4); **D**, r-Wnt3a (n=4); and **F**, BIO (n=6) revealed decreased growth capacity of CSP cells. T-cell factor–luciferase activity is measured in relative light units (RLU). Analysis of CSP cell number in **G**, the vehicle- or r-Wnt3a-injected areas (left ventricular free wall) (vehicle, n=14; r-Wnt3a, n=16), and in **H**, the remote areas from the injection sites (atria, septum, right ventricle) (vehicle, n=12; r-Wnt3a, n=13). Data are mean±SEM. \* $P\leq 0.05$  all samples to respective vehicle, # $P\leq 0.05$ , Wnt 10% to Wnt 30%; BIO, 1  $\mu\text{mol/L}$  to BIO 2  $\mu\text{mol/L}$  and BIO 5  $\mu\text{mol/L}$ ; § $P\leq 0.05$ , BIO 2  $\mu\text{mol/L}$  to BIO 5  $\mu\text{mol/L}$ . Cell number in fold change presented in **B**, **D**, and **F** is normalized to respective vehicle group.

Bromindirubin-3'-oxime), a GSK-3 inhibitor, caused a comparable decline in CSP cell number with corresponding activation of the Wnt pathway (Figure 1E and 1F). We further examined the antiproliferative effects of Wnt signaling on CSP cells in vivo, with direct intramyocardial injection of r-Wnt3a protein into the LV free wall of normal adult mouse hearts. Injection of r-Wnt3a substantially reduced the number of CSP cells (Figure 1G) in the injected area relative to vehicle, whereas the number of CSP cells remote to the injection site (atria, septum and right ventricle) remained unchanged (Figure 1H).

### Wnt3a Directly Alters the Cell Cycle Progression of Adult CSP Cells

To further investigate the antiproliferative effect of canonical Wnt signaling on CSP cells, we examined the effect of Wnt3a on cell cycle progression in CSP cells. Treatment of CSP cells with Wnt3a-CM led to a drastic reduction of cells residing in the cell cycle S phase, as evidenced by decreased BrdU incorporation (Figure 2A through 2C). Moreover, activation of canonical Wnt signaling decreased the fraction of CSP cells residing in the cell cycle M phase, as shown by immunostaining for the phosphorylated form of histone H3



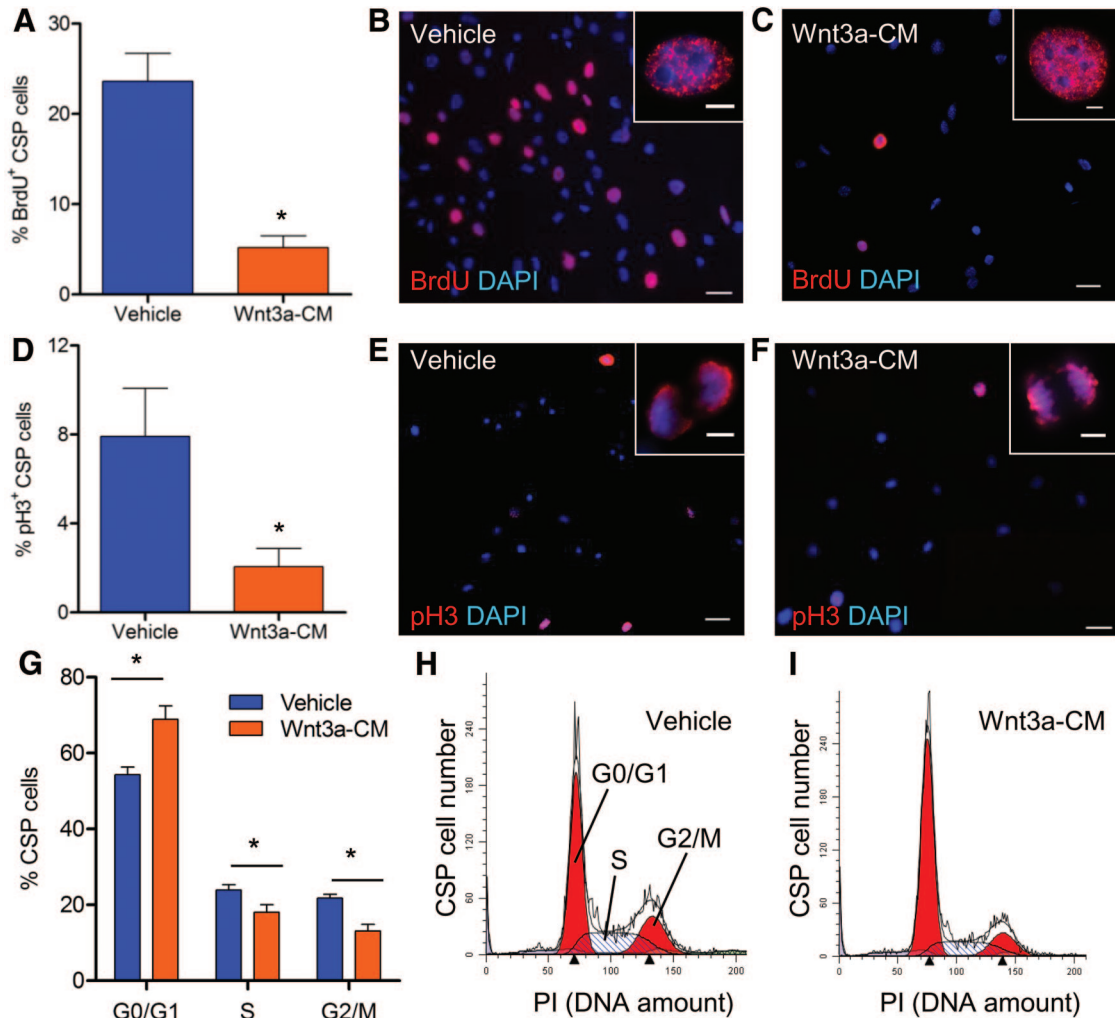


**Figure 2. Activation of the canonical Wnt signaling pathway in CSP cells blocks cell cycle progression.** Immunocytochemical analysis of **A**, BrdU incorporation ( $n=5$ ), and **D**, expression of p-H3 ( $n=4$ ) in CSP cells, after treatment with Wnt3a-conditioned medium (Wnt3a-CM) or vehicle. Representative images of **(B and C)** BrdU<sup>+</sup> and **(E and F)** p-H3<sup>+</sup> CSP cells, in low (scale bars, 50  $\mu\text{m}$ ) and high magnification (inset, scale bars, 5  $\mu\text{m}$ ). **G**, Flow cytometric analysis of CSP cells stained with propidium iodide (PI) ( $n=4$ ). Representative examples of PI analysis after treatment with vehicle **(H)** or Wnt3a-CM **(I)**. Data are mean  $\pm$  SEM. \* $P \leq 0.05$ .

(p-H3) (Figure 2D through 2F). The altered cell cycle profile in Wnt3a-CM-treated CSP cells was further tested by direct measurement of DNA content with propidium iodide staining. As demonstrated in Figure 2G through 2I, Wnt3a-CM treatment considerably increased the amount of cells residing in G0/G1-cell cycle phases while decreasing the fraction of cells residing in S- and G2/M-cell cycle phases, in comparison to vehicle treated CSP cells.

To further clarify the role of Wnt signaling in the regulation of CSP cell cycle progression, we examined the expression pattern of known cell cycle regulator genes. Consistent with the impaired proliferative capacity, treatment of CSP cells with Wnt3a-CM, in comparison to vehicle, downregulated the expression of several positive cell-cycle regulators including Ki67, PCNA, and Brca2, while upregulating negative cell-cycle regulators such as Gadd45a and p16 (Cdkn2a), within 8 hours (Online Table I). Notably, this gene expression pattern persisted throughout later time points and was accompanied by further downregulation of additional cell cycle regulators, including c-myc, Ccnf, Ccnb1, Cdk4,

Mcm3, Mcm2, Cdc25a, Brca1, and Wee1 (Online Table I). These findings suggest that canonical Wnt stimulation impairs the proliferation of adult cardiac progenitor cells potentially through modulation of cell-cycle regulators.

### IGFBP3 Is Upregulated in Response to Activated Wnt Signaling in CSP Cells

Using an RT-PCR-based array to monitor several key intracellular signaling pathways, we sought to identify possible mediators for the antiproliferative action of Wnt signaling. Several genes previously identified to be associated with Wnt signaling activation (Wnt2, Tcf7, Lef1) and with cell-cycle regulation (p16) were found to be significantly upregulated in Wnt3a-CM-treated CSP cells in comparison to vehicle-treated cells (Online Figure II, A, and Online Table II). Interestingly, among those genes examined, IGFBP3 exhibited the most robust upregulation with Wnt activation, increasing more than 40-fold (Online Figure II, A). Furthermore, IGFBP3 gene expression was upregulated by Wnt3a-CM in CSP cells in a time-dependent manner (Figure

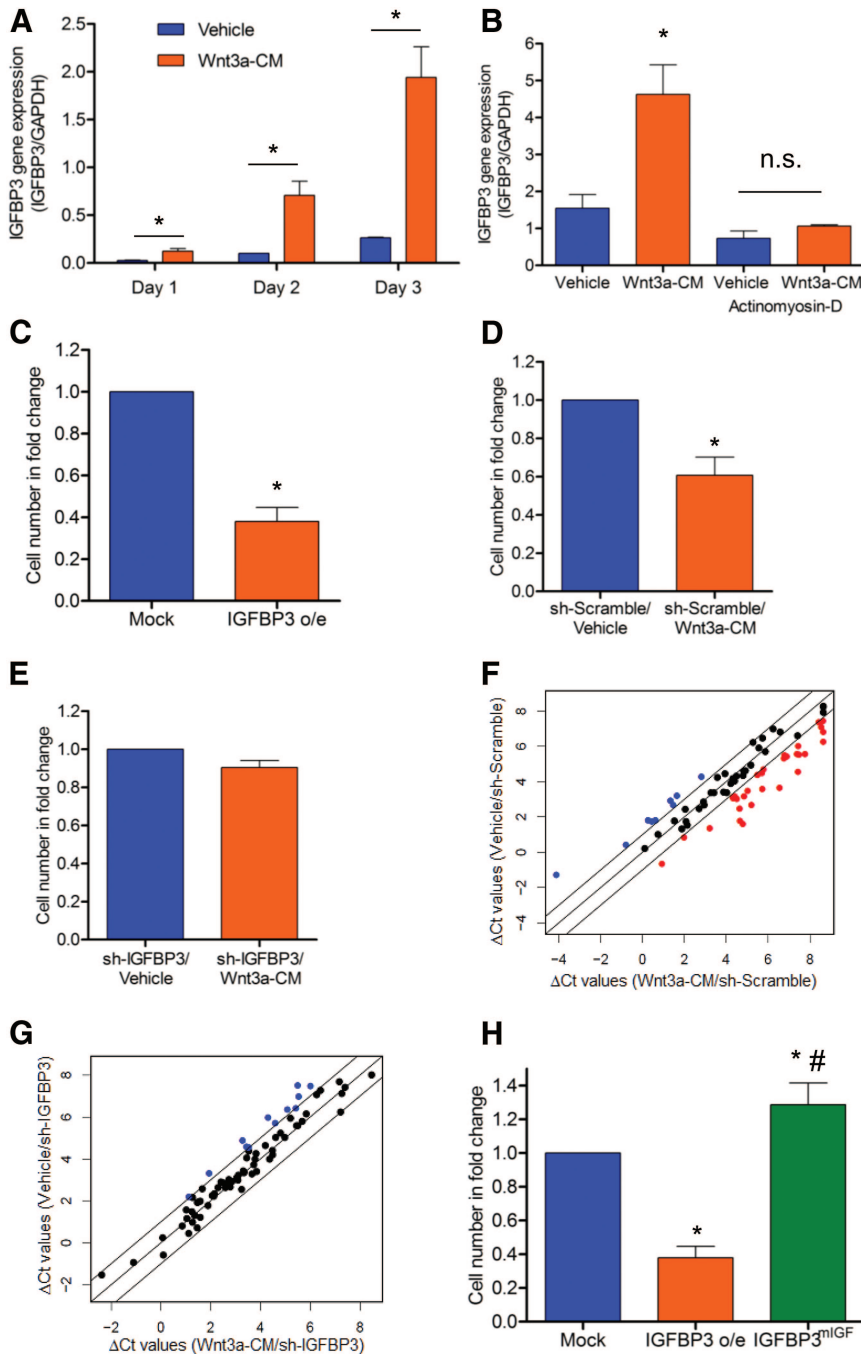


**Figure 3. IGFBP3 mediates antiproliferative effects of the Wnt signaling pathway on CSP cells.** **A**, Time course gene expression analysis of IGFBP3 in CSP cells after treatment with vehicle or Wnt3a-CM (n=3). **B**, IGFBP3 gene expression analysis in CSP cells after pretreatment with Actinomycin-D (30 minutes) and subsequent application of vehicle or Wnt3a-CM (24 hours) (n=3). **C**, Proliferation assay of mock and IGFBP3 (IGFBP3 o/e)-infected CSP cells (n=5). Proliferation assay of sh-Scramble (**D**) and sh-IGFBP3-infected (**E**) CSP cells (n=4) after treatment with vehicle or Wnt3a-CM. Scatterplot analysis of the  $\Delta$ Ct values of cell cycle-related genes, in sh-Scramble (**F**) and sh-IGFBP3-infected (**G**) CSP cells, after treatment with vehicle or Wnt3a-CM for 5 days. Outer diagonal lines indicate 2-fold changes. **Black, blue, and red circles** represent unchanged, upregulated, and downregulated genes after Wnt activation, respectively. **H**, Proliferation assay of mock, IGFBP3 o/e, and IGFBP3<sup>mIGF</sup>-infected CSP cells (n=3). Data are mean  $\pm$  SEM. \* $P \leq 0.05$  to respective vehicle or mock, # $P \leq 0.05$  IGFBP3<sup>mIGF</sup> to IGFBP3 o/e. Cell number in fold change presented in **B**, **C**, **D**, and **G** was normalized to respective vehicle or mock.

3A). Consistent to the increased gene expression, IGFBP3 protein levels were found increased in CSP cells treated with Wnt3a-CM (Online Figure II, B). To examine whether increased IGFBP3 was derived from de novo transcription, stabilization of IGFBP3 mRNA, or by alternative mechanisms, CSP cells were treated with actinomycin-D, an inhibitor of de novo transcription. Actinomycin-D abolished Wnt-mediated upregulation of IGFBP3, suggesting that the IGFBP3 induction after Wnt3a treatment was mediated predominantly by transcriptional mechanisms (Figure 3B). These experiments identify IGFBP3 as a potential mediator of Wnt3a signaling in adult cardiac progenitor cells.

### IGFBP3 Is Sufficient to Inhibit the Proliferative Capacity of CSP Cells

To test whether the expression of IGFBP3 was sufficient to mimic the antiproliferative effects of Wnt3a, we constructed a lentiviral-vector overexpressing IGFBP3 (IGFBP3 o/e) in CSP cells (Online Figure III). We found that the proliferative capacity of CSP cells overexpressing IGFBP3 was markedly decreased (Figure 3C). Consistent with this observation, overexpression of IGFBP3 resulted in a cell cycle gene expression pattern similar to that of canonical Wnt signaling, with approximately 80% of examined genes (66 genes of a total of 84 genes tested) similarly regulated in both experi-



mental conditions (Online Table III). Overall, our data suggest that IGFBP3 acts as a mediator of Wnt signaling that is sufficient to recapitulate the phenotypic response to Wnt activation in CSP cells.

### IGFBP3 Is Required for Wnt3a-Mediated Antiproliferative Effects in CSP Cells

To determine whether IGFBP3 is required for the antiproliferative effects of Wnt3a, we decreased IGFBP3 protein expression in CSP cells by using lentiviral-mediated expression of a shRNA targeting IGFBP3 (sh-IGFBP3) (Online Figure IV) before Wnt activation. Scramble-infected (sh-Scramble) CSP cells treated with Wnt3a-CM exhibited decreased proliferation (Figure 3D), similar to uninfected cells. In contrast, silencing of IGFBP3 prevented Wnt-mediated inhibition of CSP cell proliferation (Figure 3E). To further investigate the role of IGFBP3 in mediating the antiproliferative effects of Wnt signaling at the gene level, we compared the expression profile of cell cycle-related genes in sh-Scramble and sh-IGFBP3 CSP cells after treatment with vehicle or Wnt3a-CM. In sh-Scramble CSP cells, 40 of the 75 (53%) expressed cell-cycle related genes were altered (upregulated or downregulated) by more than 2-fold after treatment with Wnt3a-CM (Figure 3F and Online Table IV), including upregulation of cell-cycle inhibitors (Cdkn2a and Cdkn1a) and downregulation of positive mediators of cell-cycle progression (Ccn2, Ccnb1, E2f3, Ki67, PCNA, Mcm2, Mcm3, Mcm4, and Wee1). In sh-IGFBP3 CSP cells, only 12 of the 75 examined cell cycle regulators (16%) were altered by more than 2-fold after treatment with Wnt3a-CM (Figure 3G and Online Table IV). In sh-IGFBP3-infected CSP cells, Wnt signaling did not result in altered expression of negative cell-cycle regulators and even upregulated the expression of several positive regulators (Ccn2, Ccnb1, Wee1). Overall, our data suggest that silencing of IGFBP3 results in normalization of cell cycle gene expression in response to Wnt signaling activation and that IGFBP3 is necessary for the antiproliferative effects of Wnt3a activation in adult CSP cells.

### Integrity of IGF-Binding Site Is Required for the Antiproliferative Effect of IGFBP3 on CSP Cells

IGFBP3 is an abundant circulating IGF-binding protein and acts as a modulator of cell survival, cell proliferation, and cell metabolism through IGF-dependent or IGF-independent mechanisms.<sup>31</sup> IGFBP3 is known to bind IGFs both in vitro and in vivo.<sup>31</sup> IGF-1 is a potent stimulant of several cell types including adult cardiac stem cells.<sup>32</sup> We found that IGF-1 stimulates CSP cell proliferation in vitro (Online Figure V, A). However, the expression of IGF-1 receptors did not change after Wnt3a treatment (Online Figure V, B and C). To determine whether IGF binding to IGFBP3 is required for the antiproliferative effect of IGFBP3, we overexpressed wild-type IGFBP3 or mutated IGFBP3 with loss of the IGF binding site (IGFBP3<sup>miIGF</sup>) in CSP cells.<sup>33</sup> Overexpression of wild-type IGFBP3 decreased cell proliferation, whereas overexpression of IGFBP3<sup>miIGF</sup> increased cell division (Figure 3H), suggesting that the IGF binding site is critical for the antiproliferative function of IGFBP3 in CSP cells.

### Administration of r-Wnt3a Protein After MI Diminishes the Pool of Endogenous Cardiac Progenitors

After cardiac injury, CSP cell pools are acutely depleted and later renewed, in part, through enhanced proliferation of local CSP cells.<sup>26</sup> Given the context and cell-type dependency of Wnt activation in response to cardiac injury, we measured Wnt-related genes in CSP cells isolated from the myocardium 1, 3, and 7 days after coronary ligation. Using a Wnt pathway focused gene array, we established that Wnt-related genes were downregulated in CSP cells early after MI and continued to decline over 7 days. Conversely, a corresponding increase in Wnt pathway inhibitor genes was detected (Figure 4A through 4C and Online Tables V through VIII). During this early post-MI period, CSP proliferation increased, as shown by BrdU labeling (Figure 4D). To determine whether activation of Wnt signaling may inhibit the growth capacity of CSP cells after tissue injury, r-Wnt3a was injected into the infarct and border zone of mouse hearts after MI. Injection of r-Wnt3a after MI upregulated Wnt target genes, including *Ccnd1*, *Tcf7*, *Lef-1*, and *Wnt3a* (Figure 5A), confirming the activation of canonical Wnt in vivo. Administration of r-Wnt3a resulted in a significant reduction in CSP cell number in the region of injection (Figure 5B) but did not alter CSP cell number in areas remote to the injection site (atria, right ventricle and septum) relative to vehicle treated animals (Figure 5C). To further determine whether the Wnt-mediated decrease in CSP pools alters myocardial regeneration after MI, we determined the formation of new cardiomyocytes by pulsing BrdU, a thymidine analog, through Alzet mini-osmotic pumps for a period of 1 week. BrdU-positive cardiomyocytes were found to reside primarily in the infarct and border zone areas of the injured myocardium (Figure 6A) and were significantly decreased after r-Wnt3a administration compared with vehicle injected counterparts (Figure 6B), suggesting an impairment in new cardiomyocyte generation. Notably, the majority of BrdU-positive cardiomyocytes were smaller in size in both r-Wnt3a and vehicle-injected hearts as compared with nondividing, BrdU-negative cardiomyocytes (Figure 6C). A representative cluster of BrdU-positive cardiomyocytes located in the infarct/border zone area is presented in Online Figure VI. Our data show that activation of Wnt signaling pathway diminishes the endogenous repair mechanisms of the heart after MI.

### Administration of Wnt or IGFBP3 Adversely Affects Post-MI Cardiac Remodeling

We further determined whether diminished CSP pools and myocardial regeneration after MI influence the development of adverse cardiac remodeling. One week after MI, heart weight/body weight (Figure 7A) and infarct size (Figure 7B) were significantly increased with r-Wnt3a injection. Moreover, injection of r-Wnt3a protein and impaired myocardial regeneration were associated with decreased intraventricular septal wall thickness, increased left ventricular chamber dimension, and impaired cardiac performance, marked by reduced ratio of fractional shortening and fractional area change, compared with vehicle-injected mice (Figure 7C through 7F). Taken together, our data suggest that activation

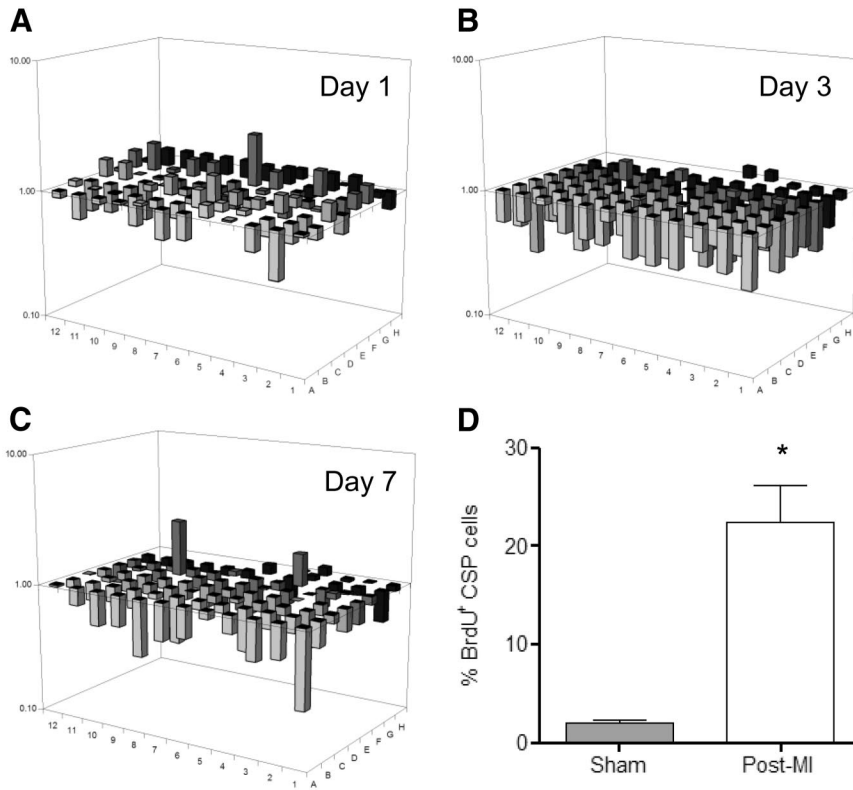


**Figure 4. Wnt signaling pathway expression profile in CSP cells after MI.** Three-dimensional diagrams show expression profile of Wnt signaling-related genes in CSP cells at 1 day after MI (A), 3 days after MI (B), and 7 days after MI (C) (n=3). The gene corresponding to each bar can be found in Online Table VIII. The position (well) A1 in (A) through (C) is located in the bottom right corner of each diagram. D, Analysis of CSP cell proliferation (BrdU incorporation assay) at 4 days after MI (n=3). Data are mean±SEM. \*P≤0.05.

of Wnt signaling worsens the post-MI structural and functional remodeling. Similarly, administration of r-IGFBP3 into the infarct/border zone area acutely after coronary artery occlusion resulted in a decrease in intraventricular septal

thickness and an increase in left ventricular chamber dimension, as well as a corresponding reduction in LV fractional shortening and fractional area change (Figure 8A through 8D). Collectively, these data suggest that IGFBP3 mimics the

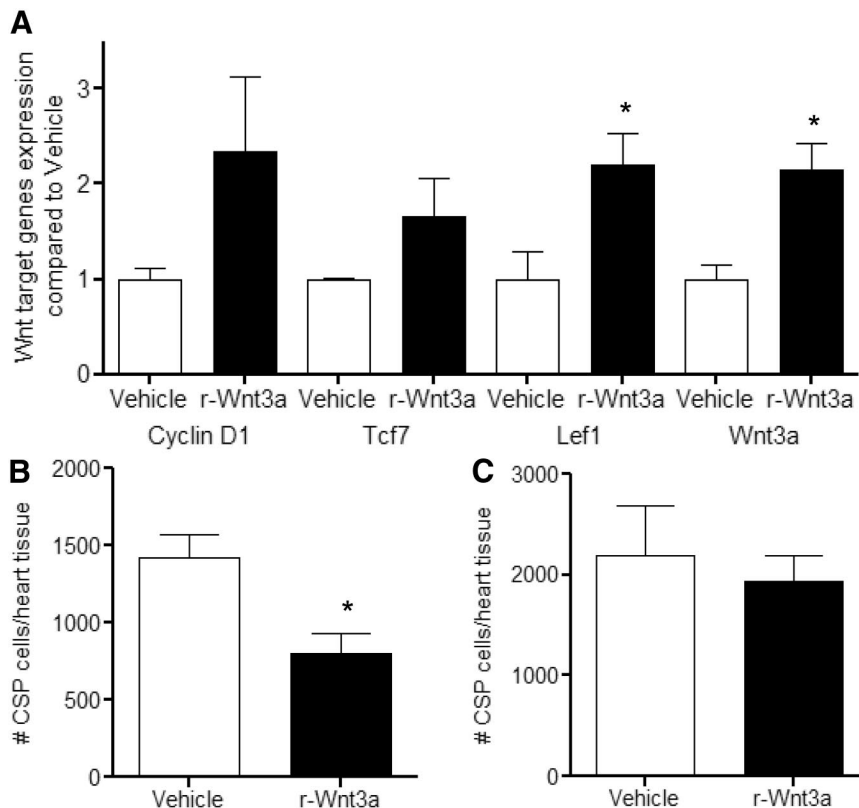


**Figure 5. Administration of r-Wnt3a protein decreases the amount of CSP cells after MI.** A, Gene expression analysis of Wnt target genes (Cyclin-D1, Tcf7, Lef1, and Wnt3a) in the infarct/border zone area (injection site) after intramyocardial injection of r-Wnt3a protein (n=3). Analysis of CSP cell number 3 days after MI, in B, the infarct/border zone area (injection site), and C, the remote areas (atria, septum, right ventricle) of vehicle-injected or r-Wnt3a-injected hearts (vehicle, n=10, and r-Wnt3a, n=9). Data are mean±SEM. \*P≤0.05.

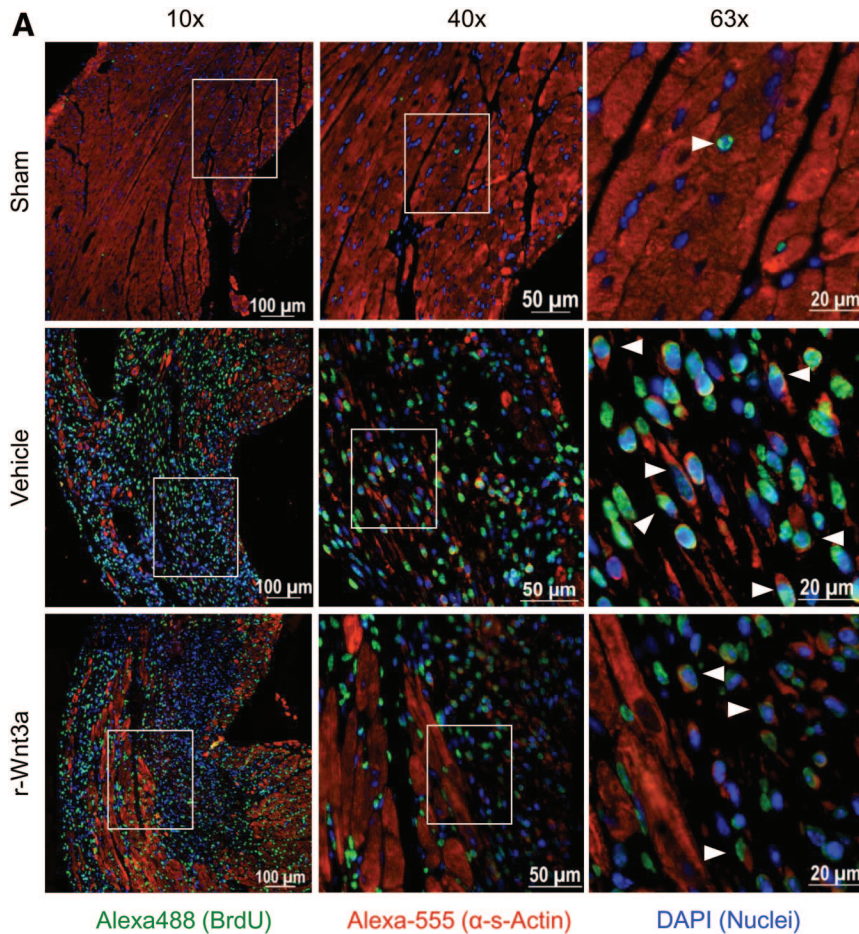
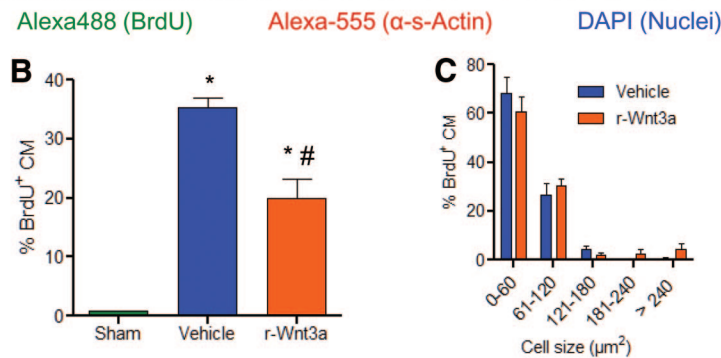


**Figure 6. Injection of r-Wnt3a after MI inhibits the formation of new cardiomyocytes (CM).** **A**, Representative fluorescent microscope images of BrdU<sup>+</sup> CM located in the infarct/border zone area 1 week after MI, presented in low (10×), medium (40×), and high (63×) magnification power. **White arrowheads**, shown in 63× magnification, indicate BrdU<sup>+</sup> CM. **B**, Quantification of BrdU incorporation in CM at 1 week after MI in sham (n=3), vehicle-injected (n=5), and r-Wnt3a-injected (n=4) hearts. **C**, Cell size distribution frequency of BrdU<sup>+</sup> CM in the infarct/border zone area of vehicle (n=3) and r-Wnt3a-injected (n=4) animals. Data are mean±SEM. \*P≤0.05, all samples to sham; #P≤0.05, r-Wnt3a to vehicle.



effects of r-Wnt3a on cardiac function in the presence of ischemic myocardial injury.

### Discussion

Detailed knowledge of the molecular cues that regulate progenitor cell fate decisions in physiological and pathological states is of the utmost importance for achieving the overarching goal of therapeutic cardiac regeneration. Wnt signaling is a pivotal factor in the regulation of organogenesis from embryonic development to aging, as well as in various disease conditions.<sup>9,10</sup> Although Wnt signaling is undoubtedly established to be critical for cardiogenesis during cardiac development,<sup>11</sup> its role in adult cardiac progenitor cells and post-MI remodeling remains poorly understood. In this study, we define the role of canonical Wnt signaling in regulating the function of adult cardiac progenitor cells *in vitro* and *in vivo*.

Furthermore, we identify a previously unknown link between canonical Wnt signaling and IGFBP3 and demonstrate an important role for IGFBP3 in mediating Wnt signaling effects in adult cardiac progenitor cells. Last, our study emphasizes the functional significance of adult cardiac progenitor cells in tissue regeneration after cardiac injury such as MI.

The antiproliferative effects of Wnt signaling on CSP cells appear to be mediated through its negative effects on the cell cycle progression. Activation of Wnt signaling leads to accumulation of CSP cells in the early nonproliferating G0/G1 cell-cycle phases, while altering substantially the expression profile of various cell cycle regulators. In contrast, prior reports suggest that Wnt signaling potentiates the expansion of embryonic and neonatal Isl-1<sup>+</sup> cardiac progenitor cells.<sup>18–20</sup> The distinct response of CSP cells to Wnt



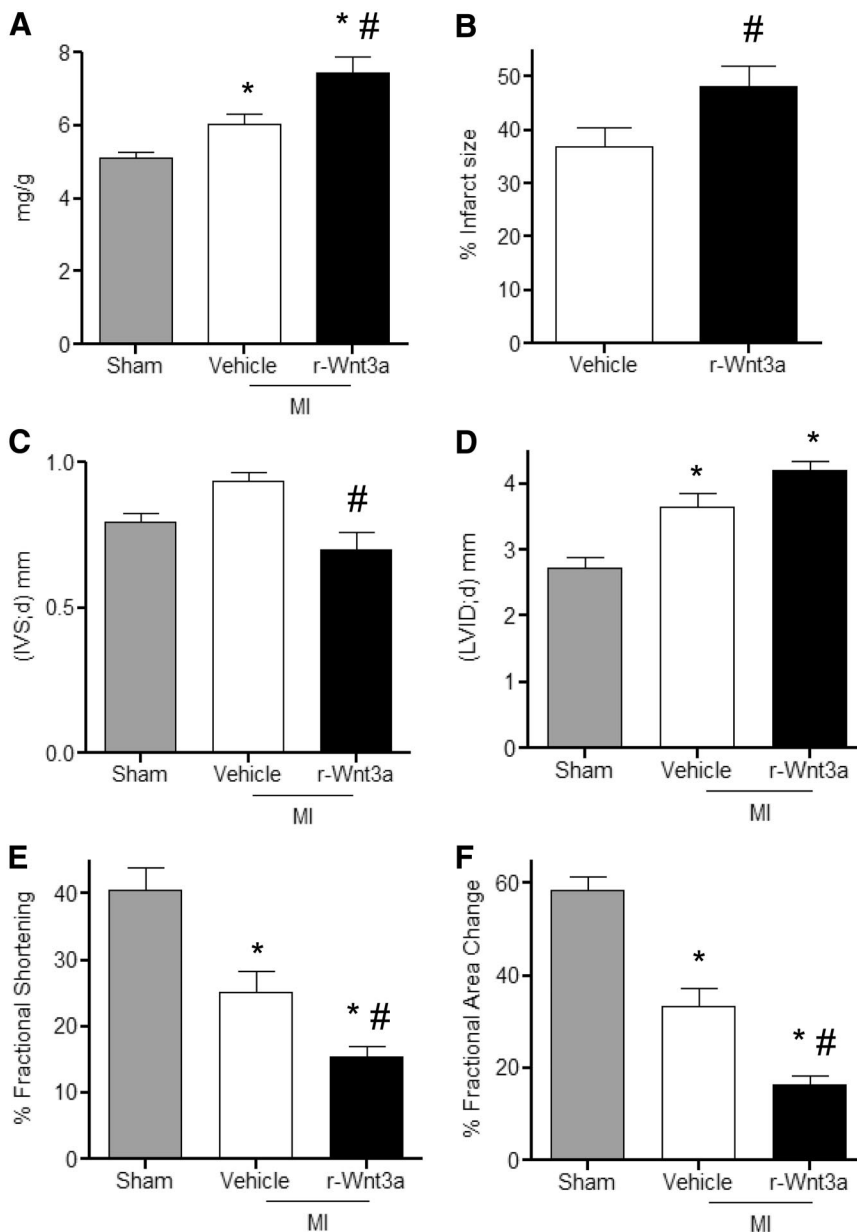


**Figure 7. Administration of r-Wnt3a after MI leads to impaired cardiac performance.** **A**, Quantification of heart weight-to-body weight ratios in sham (n=8), vehicle-injected (n=12), and r-Wnt3a-injected animals (n=12). **B**, Measurement of infarct size in vehicle and r-Wnt3a-injected hearts (n=8). Echocardiographic assessment of **C**, intraventricular septal thickness in diastole (IVS;d); **D**, left ventricular internal dimension in diastole (LVID;d); **E**, fractional shortening; and **F**, fractional area change (sham, n=7; vehicle, n=9; r-Wnt3a, n=10). All measurements were performed at 1 week after MI. Data are mean±SEM. \* $P\leq 0.05$ , all samples to sham; # $P\leq 0.05$ , r-Wnt3a to vehicle.

signals in adult versus embryonic progenitor cells probably is due to intrinsic differences of each cell type and to the highly time and context dependent nature of Wnt signaling.<sup>11,17</sup> The milieu-dependent role of Wnt signaling is also supported by recent evidence in the cancer biology field. Although Wnt signaling is associated with oncogenic transformation, it has recently been suggested that activation of Wnt signaling may decrease proliferation in melanoma cancerous cells.<sup>34</sup>

Further, we demonstrated that IGFBP3 is transcriptionally upregulated by Wnt signaling and that it is the critical determinant of the antiproliferative effects of Wnt on CSP cells. Importantly, this phenomenon depends on a functional IGF binding site in IGFBP3. Analysis of the IGFBP3 gene promoter sequence has revealed a number of conserved transcriptional factor binding sites for factors such as REPIN1, MYOD1, and NFATC.<sup>35-37</sup> ChIP-chip and ChIP-seq experiments have recognized a number of other transcrip-

tional factors that may bind to the promoter region of IGFBP3.<sup>38</sup> Recent reports suggest IGFBP5 is a potential target of Wnt-mediated transcriptional activity.<sup>39,40</sup> Among the members of the IGFBP family, IGFBP3 has a high structural and functional resemblance to IGFBP5,<sup>41,42</sup> raising the possibility that IGFBP3 is upregulated in CSP cells through a direct Wnt-mediated transcriptional mechanism.

The role of IGFBP proteins in the adult myocardium is largely unknown. The insulin-like growth factor axis (ratio of IGF-1 to IGFBP3) has been introduced as a predictor of clinical outcomes in heart failure patients.<sup>43</sup> Moreover, mice overexpressing IGFBP3 exhibited cardiac organomegaly.<sup>44</sup> More recently, a direct link between cardiomyogenesis, IGFBP proteins, and Wnt signaling was identified.<sup>45</sup> IGFBP4 increases the cardiomyogenic differentiation of P19CL6 cells and embryonic stem cells through inhibition of canonical Wnt.<sup>45</sup> However, IGFBP4 activates Wnt/ $\beta$ -catenin transcrip-

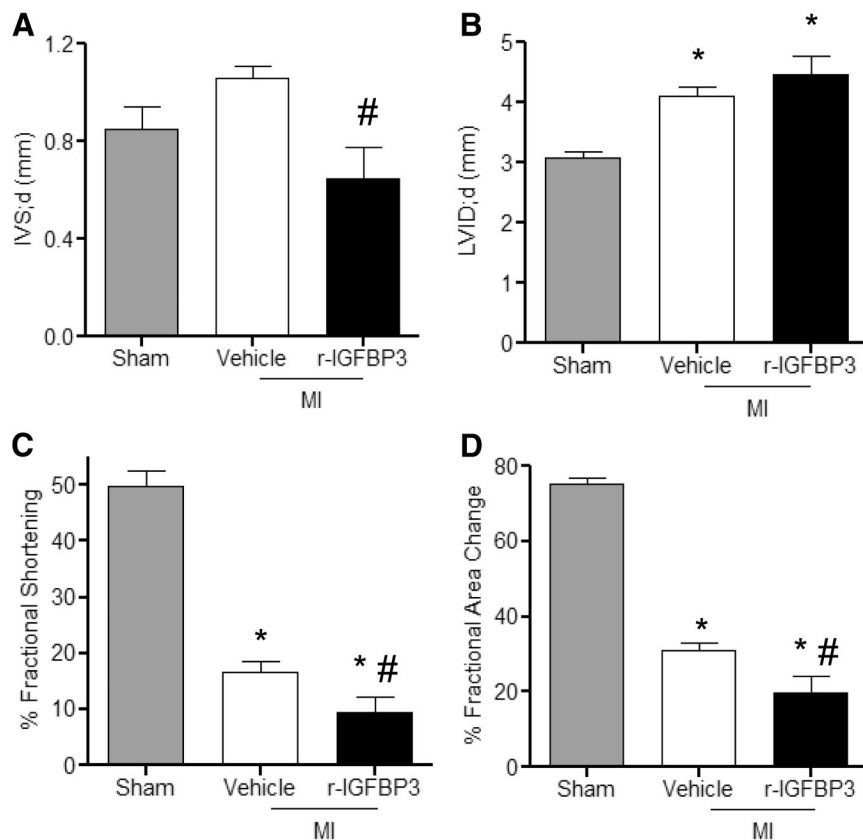


**Figure 8. Administration of r-IGFBP3 after MI compromises cardiac function.** Echocardiographic assessment of **A**, intraventricular septal thickness in diastole (IVS;d); **B**, left ventricular internal dimension in diastole (LVID;d); **C**, fractional shortening; and **D**, fractional area change (sham, n=3; vehicle, n=6; r-IGFBP3, n=6). All measurements were performed at 1 week after MI. Data are mean $\pm$ SEM. \* $P\leq 0.05$ , all samples to sham; # $P\leq 0.05$ , r-IGFBP3 to vehicle.

tional activity in a renal cancer cell line.<sup>46</sup> Thus, a context-dependent and cell type-dependent specificity may define the interaction between IGFBP proteins and Wnt.

Activation of Wnt signaling decreases resident cardiac progenitor cell renewal and negatively affects the myocardial response to infarction. SFRP1 and SFRP2, 2 well-documented Wnt signaling inhibitors, exert a potent cardioprotective effect after ischemic myocardial injury.<sup>47–50</sup> Similarly, depletion of  $\beta$ -catenin attenuates post-MI cardiac remodeling and improves animal survival by stimulating the resident cardiac stem cell pool.<sup>51</sup> Wnt signaling has been reported to be enhanced within the infarct-border zone, but Wnt activation was limited to endothelial cells, smooth muscle cells, CD31<sup>+</sup>/Sca1<sup>+</sup> cells, c-kit<sup>+</sup>/CD45<sup>+</sup> cells, and fibroblasts.<sup>52,53</sup> Results from the current study, however, indicate that Wnt pathway genes were decreased in CSP cells isolated from the infarcted heart, whereas Wnt inhibitors, such as SFRP2, increased. Consistent with this observation, we found that CSP cell proliferation was enhanced early after MI. Conversely, activation of Wnt signaling in CSP cells through the delivery of recombinant Wnt protein decreased the number of CSP cells. On the basis of in vitro data, it is reasonable to speculate that downregulation of Wnt signaling in CSP cells may promote the proliferation of CSP cells after cardiac injury. In addition to the effects on cardiac progenitor cells, r-Wnt3a may influence other cell types, including cardiomyocytes. Indeed, we found that r-Wnt3a leads to an increase in cardiomyocyte death (Online Figure VII, A), but no change is observed in cell death when all cardiac cells are considered (Online Figure VII, B). Importantly, recombinant

Wnt3a results in an increase in heart weight-to-body weight ratio, although cardiomyocyte cross-sectional area remains unchanged. These results do not exclude an increase in myocyte length, which may contribute to the expansion in cavity volume (Online Figure VIII). Although we cannot exclude that Wnt affects other cell types, our findings point to a potential interaction between impaired progenitor cell function and negative outcome after MI. Importantly, future research is necessary to determine those cell types which underlie the in vivo effects of recombinant Wnt administration and whether targeting Wnt may be a viable therapeutic option.

In summary, our work reveals a novel role of Wnt signaling pathway in adult cardiac progenitor cells and shows that canonical Wnt ligands compromise the self-renewal properties of CSP cells in vitro and in vivo. This phenomenon, in turn, may lead to impaired cardiac recovery after ischemic injury. Furthermore, we have identified a previously unrecognized link between Wnt signaling and IGFBP3, which together regulate cardiac progenitor cell function. Canonical Wnt contributes to negative left ventricular remodeling by interfering with the endogenous myocardial regeneration. Understanding the molecular signals that modulate tissue homeostasis and repair is important for the design of novel therapeutic strategies for the failing heart.

### Acknowledgments

We thank G. Losyev at the Cardiovascular FACS Core for assistance with SP cells sorting, S. Ngoy at the Cardiovascular Physiology Core for mouse surgery, and C. Mbah for assistance with echocardiogra-



phy measurements. We also thank B. Jiang and members of Liao laboratory for discussion.

### Sources of Funding

This study was supported in part by NIH grants (HL086967, HL093148, and HL099173) to R.L. and American Heart Association fellowship awards to A.O. (predoctoral) and J.-K.H. and M.B. (postdoctoral). G.F. and A.F.B. are supported by the Sarnoff Cardiovascular Research Foundation.

### Disclosures

None.

### References

- Beltrami AP, Barlucchi L, Torella D, Baker M, Limana F, Chimenti S, Kasahara H, Rota M, Musso E, Urbaneck K, Leri A, Kajstura J, Nadal-Ginard B, Anversa P. Adult cardiac stem cells are multipotent and support myocardial regeneration. *Cell*. 2003;114:763–776.
- Laugwitz KL, Moretti A, Lam J, Gruber P, Chen Y, Woodard S, Lin LZ, Cai CL, Lu MM, Reth M, Platoshyn O, Yuan JX, Evans S, Chien KR. Postnatal isl1+ cardioblasts enter fully differentiated cardiomyocyte lineages. *Nature*. 2005;433:647–653.
- Messina E, De Angelis L, Frati G, Morrone S, Chimenti S, Fiordaliso F, Salio M, Battaglia M, Latronico MV, Coletta M, Vivarelli E, Frati L, Cossu G, Giacomello A. Isolation and expansion of adult cardiac stem cells from human and murine heart. *Circ Res*. 2004;95:911–921.
- Oh H, Bradfute SB, Gallardo TD, Nakamura T, Gaussen V, Mishina Y, Pocius J, Michael LH, Behringer RR, Garry DJ, Entman ML, Schneider MD. Cardiac progenitor cells from adult myocardium: homing, differentiation, and fusion after infarction. *Proc Natl Acad Sci U S A*. 2003;100:12313–12318.
- Bearzi C, Rota M, Hosoda T, Tillmanns J, Nascimbene A, De Angelis A, Yasuzawa-Amano S, Trofimova I, Siggins RW, Lecapitaine N, Cascapera S, Beltrami AP, D'Alessandro DA, Zias E, Quaini F, Urbaneck K, Michler RE, Bolli R, Kajstura J, Leri A, Anversa P. Human cardiac stem cells. *Proc Natl Acad Sci U S A*. 2007;104:14068–14073.
- Pfister O, Mouquet F, Jain M, Summer R, Helmes M, Fine A, Colucci WS, Liao R. Cd31- but not cd31+ cardiac side population cells exhibit functional cardiomyogenic differentiation. *Circ Res*. 2005;97:52–61.
- Bergmann O, Bhardwaj RD, Bernard S, Zdunek S, Barnabe-Heider F, Walsh S, Zupicich J, Alkass K, Buchholz BA, Druid H, Jovinge S, Frisen J. Evidence for cardiomyocyte renewal in humans. *Science*. 2009;324:98–102.
- Hsieh PC, Segers VF, Davis ME, MacGillivray C, Gannon J, Molkenin JD, Robbins J, Lee RT. Evidence from a genetic fate-mapping study that stem cells refresh adult mammalian cardiomyocytes after injury. *Nat Med*. 2007;13:970–974.
- Chien AJ, Conrad WH, Moon RT. A Wnt survival guide: from flies to human disease. *J Invest Dermatol*. 2009;129:1614–1627.
- Cohen ED, Tian Y, Morrissey EE. Wnt signaling: an essential regulator of cardiovascular differentiation, morphogenesis and progenitor self-renewal. *Development*. 2008;135:789–798.
- Gessert S, Kuhl M. The multiple phases and faces of Wnt signaling during cardiac differentiation and development. *Circ Res*. 2010;107:186–199.
- Marvin MJ, Di Rocco G, Gardiner A, Bush SM, Lassar AB. Inhibition of Wnt activity induces heart formation from posterior mesoderm. *Genes Dev*. 2001;15:316–327.
- Schneider VA, Mercola M. Wnt antagonism initiates cardiogenesis in *xenopus laevis*. *Genes Dev*. 2001;15:304–315.
- Nakamura T, Sano M, Songyang Z, Schneider MD. A Wnt- and beta-catenin-dependent pathway for mammalian cardiac myogenesis. *Proc Natl Acad Sci U S A*. 2003;100:5834–5839.
- Wu X, Golden K, Bodmer R. Heart development in *Drosophila* requires the segment polarity gene *wingless*. *Dev Biol*. 1995;169:619–628.
- Naito AT, Shiojima I, Akazawa H, Hidaka K, Morisaki T, Kikuchi A, Komuro I. Developmental stage-specific biphasic roles of Wnt/beta-catenin signaling in cardiomyogenesis and hematopoiesis. *Proc Natl Acad Sci U S A*. 2006;103:19812–19817.
- Ueno S, Weidinger G, Osugi T, Kohn AD, Golob JL, Pabon L, Reinecke H, Moon RT, Murry CE. Biphasic role for Wnt/beta-catenin signaling in cardiac specification in zebrafish and embryonic stem cells. *Proc Natl Acad Sci U S A*. 2007;104:9685–9690.
- Cohen ED, Wang Z, Lepore JJ, Lu MM, Taketo MM, Epstein DJ, Morrissey EE. Wnt/beta-catenin signaling promotes expansion of isl1-positive cardiac progenitor cells through regulation of FGF signaling. *J Clin Invest*. 2007;117:1794–1804.
- Qyang Y, Martin-Puig S, Chiravuri M, Chen S, Xu H, Bu L, Jiang X, Lin L, Granger A, Moretti A, Caron L, Wu X, Clarke J, Taketo MM, Laugwitz KL, Moon RT, Gruber P, Evans SM, Ding S, Chien KR. The renewal and differentiation of isl1+ cardiovascular progenitors are controlled by a Wnt/beta-catenin pathway. *Cell Stem Cell*. 2007;1:165–179.
- Bu L, Jiang X, Martin-Puig S, Caron L, Zhu S, Shao Y, Roberts DJ, Huang PL, Dornan IJ, Chien KR. Human isl1 heart progenitors generate diverse multipotent cardiovascular cell lineages. *Nature*. 2009;460:113–117.
- Goodell MA, Brose K, Paradis G, Conner AS, Mulligan RC. Isolation and functional properties of murine hematopoietic stem cells that are replicating in vivo. *J Exp Med*. 1996;183:1797–1806.
- Challen GA, Little MH. A side order of stem cells: the sp phenotype. *Stem Cells*. 2006;24:3–12.
- Hierlihy AM, Seale P, Lobe CG, Rudnicki MA, Megeney LA. The post-natal heart contains a myocardial stem cell population. *FEBS Lett*. 2002;530:239–243.
- Oyama T, Nagai T, Wada H, Naito AT, Matsuura K, Iwanaga K, Takahashi T, Goto M, Mikami Y, Yasuda N, Akazawa H, Uezumi A, Takeda S, Komuro I. Cardiac side population cells have a potential to migrate and differentiate into cardiomyocytes in vitro and in vivo. *J Cell Biol*. 2007;176:329–341.
- Pfister O, Oikonomopoulos A, Sereti KI, Sohn RL, Cullen D, Fine GC, Mouquet F, Westerman K, Liao R. Role of the ATP-binding cassette transporter *abcg2* in the phenotype and function of cardiac side population cells. *Circ Res*. 2008;103:825–835.
- Mouquet F, Pfister O, Jain M, Oikonomopoulos A, Ngoy S, Summer R, Fine A, Liao R. Restoration of cardiac progenitor cells after myocardial infarction by self-proliferation and selective homing of bone marrow-derived stem cells. *Circ Res*. 2005;97:1090–1092.
- Jain M, DerSimonian H, Brenner DA, Ngoy S, Teller P, Edge AS, Zawadzka A, Wetzel K, Sawyer DB, Colucci WS, Apstein CS, Liao R. Cell therapy attenuates deleterious ventricular remodeling and improves cardiac performance after myocardial infarction. *Circulation*. 2001;103:1920–1927.
- Bauer M, Cheng S, Jain M, Ngoy S, Theodoropoulos C, Trujillo A, Lin FC, Liao R. Echocardiographic speckle-tracking-based strain imaging for rapid cardiovascular phenotyping in mice. *Circ Res*. 2011;108:908–916.
- Jones SE, Jomary C. Secreted frizzled-related proteins: searching for relationships and patterns. *Bioessays*. 2002;24:811–820.
- Biechele TL, Moon RT. Assaying beta-catenin/TCF transcription with beta-catenin/TCF transcription-based reporter constructs. *Methods Mol Biol*. 2008;468:99–110.
- Yamada PM, Lee KW. Perspectives in mammalian *igfbp-3* biology: local vs systemic action. *Am J Physiol Cell Physiol*. 2009;296:C954–C976.
- D'Amario D, Cabral-Da-Silva MC, Zheng H, Fiorini C, Goichberg P, Steadman E, Ferreira-Martins J, Sanada F, Piccoli M, Cappetta D, D'Alessandro DA, Michler RE, Hosoda T, Anastasia L, Rota M, Leri A, Anversa P, Kajstura J. Insulin-like growth factor-1 receptor identifies a pool of human cardiac stem cells with superior therapeutic potential for myocardial regeneration. *Circ Res*. 2011;108:1467–1481.
- Buckway CK, Wilson EM, Ahlsen M, Bang P, Oh Y, Rosenfeld RG. Mutation of three critical amino acids of the n-terminal domain of IGF-binding protein-3 essential for high affinity IGF binding. *J Clin Endocrinol Metab*. 2001;86:4943–4950.
- Chien AJ, Moore EC, Lonsdorf AS, Kulikauskas RM, Rothberg BG, Berger AJ, Major MB, Hwang ST, Rimm DL, Moon RT. Activated Wnt/beta-catenin signaling in melanoma is associated with decreased proliferation in patient tumors and a murine melanoma model. *Proc Natl Acad Sci U S A*. 2009;106:1193–1198.
- Lu XF, Jiang XG, Lu YB, Bai JH, Mao ZB. Characterization of a novel positive transcription regulatory element that differentially regulates the insulin-like growth factor binding protein-3 (*igfbp-3*) gene in senescent cells. *J Biol Chem*. 2005;280:22606–22615.
- Paquette J, Bessette B, Ledru E, Deal C. Identification of upstream stimulatory factor binding sites in the human *igfbp3* promoter and potential implication of adjacent single-nucleotide polymorphisms and responsiveness to insulin. *Endocrinology*. 2007;148:6007–6018.
- Schweighofer B, Testori J, Sturtzel C, Sattler S, Mayer H, Wagner O, Bilban M, Hofer E. The Vegf-induced transcriptional response comprises

- gene clusters at the crossroad of angiogenesis and inflammation. *Thromb Haemost.* 2009;102:544–554.
38. McCabe CD, Spyropoulos DD, Martin D, Moreno CS. Genome-wide analysis of the homeobox c6 transcriptional network in prostate cancer. *Cancer Res.* 2008;68:1988–1996.
  39. Baurand A, Zelarayan L, Betney R, Gehrke C, Dunger S, Noack C, Busjahn A, Huelsken J, Taketo MM, Birchmeier W, Dietz R, Bergmann MW. Beta-catenin downregulation is required for adaptive cardiac remodeling. *Circ Res.* 2007;100:1353–1362.
  40. Chen Y, Guo Y, Ge X, Itoh H, Watanabe A, Fujiwara T, Kodama T, Aburatani H. Elevated expression and potential roles of human sp5, a member of sp transcription factor family, in human cancers. *Biochem Biophys Res Commun.* 2006;340:758–766.
  41. Burger AM, Leyland-Jones B, Banerjee K, Spyropoulos DD, Seth AK. Essential roles of igfbp-3 and igfbp-rp1 in breast cancer. *Eur J Cancer.* 2005;41:1515–1527.
  42. Hwa V, Oh Y, Rosenfeld RG. The insulin-like growth factor-binding protein (IGFBP) superfamily. *Endocr Rev.* 1999;20:761–787.
  43. Watanabe S, Tamura T, Ono K, Horiuchi H, Kimura T, Kita T, Furukawa Y. Insulin-like growth factor axis (insulin-like growth factor-I/insulin-like growth factor-binding protein-3) as a prognostic predictor of heart failure: association with adiponectin. *Eur J Heart Fail.* 2010;12:1214–1222.
  44. Murphy LJ, Molnar P, Lu X, Huang H. Expression of human insulin-like growth factor-binding protein-3 in transgenic mice. *J Mol Endocrinol.* 1995;15:293–303.
  45. Zhu W, Shiojima I, Ito Y, Li Z, Ikeda H, Yoshida M, Naito AT, Nishi J, Ueno H, Umezawa A, Minamoto T, Nagai T, Kikuchi A, Asashima M, Komuro I. Igfbp-4 is an inhibitor of canonical Wnt signalling required for cardiogenesis. *Nature.* 2008;454:345–349.
  46. Ueno K, Hirata H, Majid S, Tabatabai Z, Hinoda Y, Dahiya R. Igfbp-4 activates the Wnt/beta-catenin signaling pathway and induces m-cam expression in human renal cell carcinoma. *Int J Cancer.* 2011;129:2360–2369.
  47. Alfaro MP, Pagni M, Vincent A, Atkinson J, Hill MF, Cates J, Davidson JM, Rottman J, Lee E, Young PP. The Wnt modulator sfrp2 enhances mesenchymal stem cell engraftment, granulation tissue formation and myocardial repair. *Proc Natl Acad Sci U S A.* 2008;105:18366–18371.
  48. Mirosou M, Zhang Z, Deb A, Zhang L, Gnechhi M, Noiseux N, Mu H, Pachori A, Dzau V. Secreted frizzled related protein 2 (sfrp2) is the key akt-mesenchymal stem cell-released paracrine factor mediating myocardial survival and repair. *Proc Natl Acad Sci U S A.* 2007;104:1643–1648.
  49. Bergmann MW. Wnt signaling in adult cardiac hypertrophy and remodeling: lessons learned from cardiac development. *Circ Res.* 2010;107:1198–1208.
  50. Barandon L, Couffinhal T, Ezan J, Dufourcq P, Costet P, Alzieu P, Leroux L, Moreau C, Dare D, Duplaa C. Reduction of infarct size and prevention of cardiac rupture in transgenic mice overexpressing frza. *Circulation.* 2003;108:2282–2289.
  51. Zelarayan LC, Noack C, Sekkali B, Kmecova J, Gehrke C, Renger A, Zafiriou MP, van der Nagel R, Dietz R, de Windt LJ, Balligand JL, Bergmann MW. Beta-catenin downregulation attenuates ischemic cardiac remodeling through enhanced resident precursor cell differentiation. *Proc Natl Acad Sci U S A.* 2008;105:19762–19767.
  52. Aisagbonhi O, Rai M, Ryzhov S, Atria N, Feoktistov I, Hatzopoulos AK. Experimental myocardial infarction triggers canonical Wnt signaling and endothelial-to-mesenchymal transition. *Dis Model Mech.* 2011;4:469–483.
  53. Oerlemans MI, Goumans MJ, van Middelaar B, Clevers H, Doevendans PA, Sluijter JP. Active Wnt signaling in response to cardiac injury. *Basic Res Cardiol.* 2010;105:631–641.

## Novelty and Significance

### What Is Known?

- Cardiac side population (CSP) cells represent an endogenous pool of progenitor cells in the adult heart.
- The molecular mechanisms that dictate the homeostasis and cell fate of CSP cells remain elusive.
- Wnt signals are key molecules that govern cardiac development and proliferation of embryonic stem cells, though their role in regulating adult cardiac progenitor cells remains unknown.

### What New Information Does This Article Contribute?

- Activation of Wnt signaling pathway negatively regulates the proliferation capacity of adult CSP cells and compromises the endogenous regenerative capacity of the heart after myocardial infarction.
- Wnt stimulation exerts its antiproliferative effects through a previously unappreciated transcriptional activation of insulin-like growth factor binding protein 3 (IGFBP3).

Designing novel therapeutic approaches to modulate the endogenous regenerative capacity of the failing heart represents a

desirable, although challenging, task. Understanding the basic mechanisms that control homeostasis of cardiac precursors, such as CSP cells, is of fundamental importance in achieving this goal. The Wnt signaling pathway is a key modulator of cardiac development and a major factor that determines cell fate, particularly in embryonic stem cell populations. However, the role of Wnt signaling in adult cardiac progenitor cells remains unclear. Our work reveals an antiproliferative effect for Wnt signaling in adult CSP cells through a previously unappreciated transcriptional interaction with IGFBP3 and direct regulation of CSP cell cycle progression. After cardiac injury in vivo, Wnt signaling is downregulated in CSP cells with corresponding increase in CSP cell proliferation. Increasing Wnt stimulation after myocardial infarction in CSP cells compromises the endogenous regenerative capacity of the heart and is associated with worsening of cardiac remodeling. Our findings demonstrate that canonical Wnt signaling is a potent modulator of endogenous adult cardiac progenitor cells and suggest that modulation of Wnt signaling or IGFBP3 may be an effective therapeutic strategy for promoting cardiac regeneration.

## SUPPLEMENTAL MATERIAL

### *Detailed Methods*

**Myocardial infarction:** MI was generated via permanent coronary ligation as previously described.<sup>1</sup> C57BL/6J male mice (8-10 weeks old) were anesthetized using 65 mg/kg pentobarbital. Mice were ventilated using a standard rodent ventilator. An incision was performed between the fourth and the fifth intercostals space. After the pericardium was removed a descending coronary artery was permanently ligated with a silk suture. Sham-operated animals underwent an identical surgical operation lacking the occlusion of the coronary artery. To prevent any post-operative discomfort animals received buprenorphine (0.03-0.06 mg/kg). Immediately after myocardial infarction and injection of r-Wnt3a protein osmotic minipumps (Alzet, 1007D) were implanted subcutaneously in the back of each mouse. Each pump was loaded with BrdU dissolved in NaHCO<sub>3</sub> (150 mmol/L) buffer at a concentration of 40 mg/ml. BrdU pumps remained in place for a period of 7 days.

**Heart fixation:** Mice were anesthetized by intra-peritoneal injection of pentobarbital (65 mg/ml) followed by intra-peritoneal administration of 100 IU/ml anticoagulant heparin. Hearts were rapidly excised and washed briefly in Krebs buffer (NaCl 137 mmol/L, KCl 4.0 mmol/L, CaCl<sub>2</sub> 1.8 mmol/L, KH<sub>2</sub>PO<sub>4</sub> 1.2 mmol/L, MgSO<sub>4</sub> 1.2 mmol/L, NaHCO<sub>3</sub> 24.9 mmol/L, and dextrose 11.2 mmol/L (pH 7.4)). A short cannula was connected to the aortic root to initiate retrograde perfusion by the Langendorff apparatus. A thin cannula was pierced through the apex of the left ventricle (LV) to vent the besian drainage. A ventricular balloon was inserted into the LV through the mitral valve via an incision in the left atrium. The balloon was connected to a pressure transducer (Statham P23Db, Gould) for recording the LV pressure. Hearts were paced (Grass Instruments) with platinum wires placed on the epicardial surface of the right ventricle. Coronary perfusion pressure was held constant during the duration of the experiment at 80 mm Hg. The balloon was inflated with saline to adjust the end-diastolic pressure (EDP) to 5 mm Hg. When the end-diastolic pressure reached 5 mm Hg, hearts were arrested in diastole with KCl and were perfused with 10% buffered formalin solution at a hydrostatic pressure of 40-50 mm Hg for 15 minutes. Hearts remained overnight in 10% buffered formalin solution at 4°C. Subsequently, the balloon and the excess formalin were removed and the hearts were weighed. Hearts were imbedded in paraffin, cut in three parts (apex, middle, base) and analyzed by immuno-histochemistry.

**Echocardiography:** Echocardiograms were obtained at baseline (1 day prior coronary occlusion) and 7 days following MI, with a Vevo 2100 Imaging digital ultrasound system (VisualSonics). Echocardiography was performed using an 18-38 MHz linear-array transducer. Prior to echocardiography the chest was shaved and the animals were placed on a heated platform in the supine position. Echocardiographic analysis was performed in conscious mice at a physiological heart rate (>500 beats/minute). Data acquisition was initiated with the parasternal cardiac long axis view and subsequently with a short axis view, at the level of mid-papillary muscles. Echocardiographic measurements were performed from M-mode images. All data were acquired and analyzed in a blinded fashion.

**Immuno-histochemistry.** Formalin fixed tissue slides were deparaffinized via incubation at 65°C for 30 minutes and re-hydrated through sequential three minute incubations in xylene, ethanol (96%, 90%, 80%) and water. Antigen retrieval was performed by microwave heating in citrate buffer (0.1 M, pH 6.0) for 10 minutes. Slides were incubated with primary antibodies against BrdU (Roche) and  $\alpha$ -sarcomeric-actin (Sigma) for 1 hour at 37°C, followed by incubation with appropriate secondary antibodies at the same conditions. Slides were subsequently washed and mounted with DAPI-containing medium (Vector Vectashield). Infarct area and border zone were scanned for the presence of BrdU positive

cardiomyocytes (CM) through examination of 10-20 mosaic-pictures of each section obtained by epi-fluorescence microscopy (Zeiss, Axiovert 200M). Each mosaic picture was composed of 9-12 high power (63X) images. The ratio of BrdU<sup>+</sup> CM over total nucleated CM was calculated for every image. Confocal imaging was performed with a LSM 700 system (Zeiss). Image acquisition and analysis were performed in a blinded fashion. Myocyte cross-sectional area was assessed by staining the cardiac tissue with Alexa Fluor 555 conjugated wheat germ agglutinin (WGA) (Invitrogen). Apoptotic cell death was determined by Tunel staining (Roche) according to the instructions of the manufacturer.

**RT-PCR gene array.** RNA samples from expanded CSP cells treated with Vehicle or Wnt3a-CM (a), CSP cells infected with Mock or IGFBP3-o/e (b), CSP cells infected with sh-Scramble or sh-IGFBP3 (c) and freshly isolated CSP cells harvested from sham and post-MI (1, 3 and 7 days after injury) (d) were used for cDNA synthesis (RT<sup>2</sup>-First strand kit, SABiosciences). RT-PCR gene-arrays (SABiosciences) focused on cell-cycle regulation (a, b and c), signal transduction pathways (b) and Wnt signaling pathway (d) were performed according to the instructions of the manufacturer using a MyiQ cycler (Bio-Rad). Data were acquired from 3 independent experiments each with three replications and analysis was performed as follows:  $\Delta Ct$  values of all examined genes were obtained by subtracting the mean threshold cycle (Ct) value of 5 housekeeping genes (Gusb, Hprt1, Hsp90ab1, Gapdh, Actb) from the Ct value of each gene. Subsequently,  $\Delta\Delta Ct$  values for all genes were calculated as follows:  $\Delta\Delta Ct = \Delta Ct_{\text{experimental}} - \Delta Ct_{\text{control}}$ . Fold differences were calculated based on the formula:  $Fold\ difference = 2^{-\Delta\Delta Ct}$ .

**Production of Wnt3a conditioned medium (CM).** Vehicle-CM (Vehicle) and Wnt3a-CM were produced from L-M (TK-) cells and L-M (TK-)-Wnt3a cells according the instructions of American Type Culture Collection (ATCC).

**Cell expansion and lentiviral infection.** CSP cells were isolated as previously described<sup>2</sup> and cultured in expansion medium [ $\alpha$ -MEM (Lonza) with 20% FBS (Hyclone), 2 mmoles/L, L-Glutamine and 1% penicillin/streptomycin] at a density of 10-15 cells/mm<sup>2</sup>. CSP cells of passages 3-5 were infected with lentivirus and 48 hours later were used in proliferation assays. Lentivirus with sh-Scramble, sh-IGFBP3, empty vector (Mock), IGFBP3-o/e, IGFBP3<sup>mIGF</sup> or pBARL (TCF-controlled luciferase reporter) and pSL9 (Ef1-a-controlled Renilla luciferase control)<sup>3</sup>, were used as described in the manuscript.

**Proliferative capacity assay.** In vitro proliferation capacity of CSP cells was determined by cell counting, cell cycle markers including BrdU and phospho-Histone H3 (p-H3), and DNA content measurements through propidium iodide (PI) staining. Briefly, CSP cells were cultured at an initial density of 3.5-7 cells/mm<sup>2</sup> in our established  $\alpha$ -MEM based expansion medium with 20% FBS with various concentrations of Vehicle, Wnt3a-CM, BIO ((2',3'E)-6-Bromoindirubin-3'-oxime), IGF-1 (Peprotech), recombinant Wnt3a protein or recombinant SFRP2 (R&D). Culture medium was replaced every 72 hours and following 6 days in culture, cell number was determined using hemacytometer and flow cytometer (C6 Accuri cytometer). For immuno-cytochemistry detection, CSP cells were cultured on coverslips in expansion medium for five days. For BrdU incorporation assays, at day 5 CSP cells were pulsed with 10 $\mu$ M BrdU for 1 hour and BrdU was detected using a labeling kit (Roche) according to the instructions of the manufacturer. p-H3 (Abcam) was detected by immunocytochemical staining as previously described.<sup>4</sup> CSP cells were visualized using Zeiss epi-fluorescent microscopy. For DNA content measurements, CSP cells were fixed using 70% ethanol following 5 days culture and were stained with PI (PBS, 0.1% Triton-X 100, 2 $\mu$ g/ml PI, 400 ng/ml RNase-A) for one hour at 37°C under light-free conditions. CSP cells were analyzed by FACS and data were processed by ModFit Lt (Verity Software House).



**IGFBP-3 over-expression:** IGFBP-3 cDNA was excised by XbaI/XmaI enzymatic digestion from vector pSport-6 (Open Biosystems). The cDNA-fragment was blunted and ligated into lentiviral expression vector LSLV-83 (kindly provided by Dr. Paul Allen) downstream of the constitutively active promoter EF1a. Infected cells were selected with neomycin (1mg/ml) for a period of 7-10 days.

**IGFBP-3 shRNA.** pLKO.1-puro lentiviral vectors encoding Scramble or IGFBP3 (TRCN0000112128) shRNAs were obtained from Open Biosystems. CSP cells were infected with lentiviruses and selected using puromycin treatment (4µg/ml) over a period of 7-10 days.

**IGFBP-3 mutagenesis.** Lentiviral plasmid containing WT-IGFBP3 cDNA was utilized as a template for site-directed mutagenesis (quick-change mutagenesis kit, Stratagene), according to manufacturer's instructions. In brief, complementary primers encoding the desired mutations were annealed to the template LSLV-83-IGFBP3 plasmid and Pfu polymerase was used to replicate the template, incorporating the mutated primers. The template plasmid was digested with DpnI, prior to transformation. The utilized primers are as follows:

IGFBP3<sup>mIGF</sup>-sense:CCCGCTGAGGGCGGGGGGAATGGCCGCGGG

IGFBP3<sup>mIGF</sup>-antisense:CCCGCGGCCATTCCCCCGCCCTCAGCGGG.

All mutated plasmids were sequence verified.

**Cell viability assay:** Annexin-V staining (Abcam) was used to determine cell death, according to the instructions of the manufacturer, using a flow cytometer (C6 Accuri cytometer).

**Actinomyosin-D treatment:** CSP cells were treated with 5µg/ml Actinomyosin-D for a period of 30 minutes, prior to application of Vehicle or Wnt3a-CM (25%) for a period of 24 hours.

**Western blot:** Immunoblot was performed as previously described.<sup>5</sup> Primary antibodies against IGFBP3 (Santa Cruz) or GAPDH (R&D) followed by appropriate secondary antibodies (Alexa-Fluor 680, Molecular probes) were applied. All incubations were performed for two hours at room temperature under constant movement. Antibody binding was detected using the Odyssey infrared system (LI-COR).



## Online Tables

**Online Table I:** Cell cycle-focused RT-PCR gene array in CSP cells treated with Vehicle or Wnt3a-CM.

Cell cycle RT-PCR array							
Description	Symbol	8 hours ( $\Delta$ Ct)		Fold change	48 hours ( $\Delta$ Ct)		Fold Change
		Vehicle	Wnt3a- CM		Vehicle	Wnt3a- CM	
Integrin beta 1 (fibronectin receptor beta)	Itgb1	-1.87	-2.28	<b>1.33</b>	-0.14	-1.36	<b>2.33*</b>
Cyclin-dependent kinase inhibitor 2A	Cdkn2a	5.09	4.08	<b>2.00*</b>	2.52	1.49	<b>2.04*</b>
Cyclin-dependent kinase inhibitor 1A (P21)	Cdkn1a	0.17	0.34	<b>-1.12</b>	1.60	1.23	<b>1.30</b>
Peripheral myelin protein 22	Pmp22	3.11	2.99	<b>1.08</b>	1.94	1.63	<b>1.24</b>
Cyclin D1	Ccnd1	3.37	3.28	<b>1.06</b>	2.49	2.23	<b>1.20</b>
Transformed mouse 3T3 cell double minute 2	Mdm2	2.61	2.64	<b>-1.01</b>	1.65	1.39	<b>1.20</b>
DNA-damage inducible transcript 3	Ddit3	4.47	4.26	<b>1.15</b>	4.82	4.61	<b>1.16</b>
Protein phosphatase 2 (formerly 2A), regulatory subunit B", alpha	Ppp2r3a	9.88	9.90	<b>-1.01</b>	10.09	9.92	<b>1.12</b>
Adenylate kinase 1	Ak1	1.85	1.67	<b>1.13</b>	2.82	2.68	<b>1.10</b>
Protein phosphatase 1D magnesium-dependent, delta isoform	Ppm1d	4.91	5.06	<b>-1.10</b>	4.24	4.74	<b>-1.41*</b>
Structural maintenance of chromosomes 1A	Smc1a	4.70	4.62	<b>1.05</b>	3.99	4.48	<b>-1.41*</b>
Nucleophosmin/nucleoplasmin 2	Npm2	9.83	9.90	<b>-1.04</b>	9.46	9.98	<b>-1.43*</b>
Cell division cycle 25 homolog A (S. pombe)	Cdc25a	3.36	3.55	<b>-1.14</b>	4.36	4.88	<b>-1.44*</b>
Transcription factor Dp 1	Tfdp1	1.33	1.38	<b>-1.03</b>	1.04	1.60	<b>-1.48*</b>
Stromal antigen 1	Stag1	5.04	5.51	<b>-1.38</b>	4.78	5.39	<b>-1.52*</b>
Telomeric repeat binding factor 1	Terf1	6.22	6.54	<b>-1.24</b>	4.71	5.34	<b>-1.54*</b>
Cyclin B1	Ccnb1	4.54	4.46	<b>1.05</b>	3.17	3.80	<b>-1.55*</b>
Proliferating cell nuclear antigen	Pcna	1.71	2.03	<b>-1.25*</b>	0.92	1.57	<b>-1.57*</b>
Protein phosphatase 3, catalytic subunit, alpha isoform	Ppp3ca	4.67	5.07	<b>-1.31</b>	4.08	4.77	<b>-1.62*</b>

RAD21 homolog ( <i>S. pombe</i> )	Rad21	4.71	5.01	<b>-1.22</b>	1.95	2.65	<b>-1.62*</b>
Cyclin-dependent kinase 4	Cdk4	2.13	2.47	<b>-1.26</b>	1.20	1.91	<b>-1.63*</b>
Inhibin alpha	Inha	8.30	8.48	<b>-1.13</b>	7.77	8.47	<b>-1.63*</b>
Mdm2, transformed 3T3 cell double minute p53 binding protein	Mtbp	8.32	8.67	<b>-1.27</b>	5.13	5.84	<b>-1.63*</b>
Minichromosome maintenance deficient 3 ( <i>S. cerevisiae</i> )	Mcm3	2.95	3.10	<b>-1.11</b>	2.86	3.57	<b>-1.64*</b>
MutS homolog 2 ( <i>E. coli</i> )	Msh2	4.23	4.23	<b>-1.00</b>	3.80	4.54	<b>-1.66*</b>
Checkpoint kinase 1 homolog ( <i>S. pombe</i> )	Chek1	5.53	6.15	<b>-1.53</b>	5.48	6.22	<b>-1.67*</b>
RAD9 homolog ( <i>S. pombe</i> )	Rad9	5.62	5.90	<b>-1.21</b>	5.19	5.97	<b>-1.72*</b>
NIMA (never in mitosis gene a)-related expressed kinase 2	Nek2	N/A	N/A	N/A	4.28	5.07	<b>-1.73*</b>
RAD51 homolog ( <i>S. cerevisiae</i> )	Rad51	6.23	6.86	<b>-1.55</b>	4.99	5.81	<b>-1.77*</b>
MAD2 mitotic arrest deficient-like 1 (yeast)	Mad211	3.91	4.21	<b>-1.2</b>	3.28	4.12	<b>-1.79*</b>
Transformation related protein 53	Trp53	2.98	3.15	<b>-1.12</b>	1.83	2.68	<b>-1.81*</b>
Retinoblastoma-like 1 (p107)	Rbl1	5.51	5.96	<b>-1.37</b>	5.69	6.57	<b>-1.85*</b>
Myeloblastosis oncogene	Myb	N/A	N/A	N/A	12.28	13.25	<b>-1.96*</b>
Breast cancer 2	Brca2	6.72	8.67*	<b>-3.88*</b>	6.67	7.70	<b>-2.04*</b>
WEE 1 homolog 1 ( <i>S. pombe</i> )	Wee1	5.16	5.53	<b>-1.29</b>	5.24	6.27	<b>-2.04*</b>
Breast cancer 1	Brca1	6.20	6.73	<b>-1.44</b>	5.58	6.62	<b>-2.06*</b>
Cyclin F	Ccnf	4.40	4.32	<b>1.06</b>	3.71	4.76	<b>-2.06*</b>
Minichromosome maintenance deficient 2 mitotin ( <i>S. cerevisiae</i> )	Mcm2	4.23	4.47	<b>-1.18</b>	2.75	3.81	<b>-2.07*</b>
Antigen identified by monoclonal antibody Ki67	Mki67	5.02	6.59	<b>-2.96*</b>	2.94	4.07	<b>-2.19*</b>
Transformation related protein 63	Trp63	10.02	9.90	<b>1.08</b>	10.58	13.40	<b>-7.09*</b>
Calcium/calmodulin-dependent protein kinase II alpha	Camk2a	N/A	N/A	N/A	9.14	9.14	<b>-1.00</b>
Polycystic kidney disease 1 homolog	Pkd1	4.06	3.80	<b>1.20</b>	3.74	3.76	<b>-1.01</b>
Notch gene homolog 2 ( <i>Drosophila</i> )	Notch2	6.57	6.80	<b>-1.17</b>	5.23	5.29	<b>-1.04</b>
Microtubule-actin crosslinking factor 1	Macf1	2.53	2.61	<b>-1.05</b>	3.01	3.12	<b>-1.07</b>

Amyloid beta (A4) precursor protein-binding, family B, member 1	Apbb1	9.45	8.78	<b>1.59</b>	8.76	8.87	<b>-1.08</b>
Cyclin C	Ccnc	6.36	6.59	<b>-1.17</b>	7.30	7.44	<b>-1.10</b>
Tumor susceptibility gene 101	Tsg101	6.80	6.51	<b>1.22</b>	7.03	7.17	<b>-1.10</b>
Nuclear factor of activated T-cells, cytoplasmic, calcineurin-dependent 1	Nfatc1	2.99	3.02	<b>-1.01</b>	4.46	4.63	<b>-1.12</b>
RAD17 homolog (S. pombe)	Rad17	5.93	5.90	<b>1.01</b>	4.81	4.99	<b>-1.13</b>
SMT3 suppressor of mif two 3 homolog 1 (yeast)	Sumo1	2.24	2.37	<b>-1.09</b>	2.10	2.28	<b>-1.13</b>
TAF10 RNA polymerase II, TATA box binding protein (TBP)-associated factor	Taf10	2.37	2.36	<b>1.00</b>	1.31	1.53	<b>-1.16</b>
G protein-coupled receptor 132	Gpr132	N/A	N/A	N/A	12.38	12.60	<b>-1.17</b>
Sestrin 2	Sesn2	7.65	7.39	<b>1.19</b>	5.57	5.80	<b>-1.17</b>
RAN, member RAS oncogene family	Ran	-1.57	-1.44	<b>-1.09</b>	-1.58	-1.33	<b>-1.19</b>
CDK5 regulatory subunit associated protein 1	Cdk5rap1	7.71	7.14	<b>1.48</b>	7.76	8.03	<b>-1.2</b>
C-abl oncogene 1, receptor tyrosine kinase	Abl1	N/A	N/A	N/A	9.49	9.76	<b>-1.21</b>
E2F transcription factor 4	E2f4	2.73	2.93	<b>-1.15</b>	3.96	4.25	<b>-1.22</b>
Pescadillo homolog 1, containing BRCT domain (zebrafish)	Pes1	3.67	3.86	<b>-1.13</b>	2.20	2.50	<b>-1.23</b>
DnaJ (Hsp40) homolog, subfamily C, member 2	Dnajc2	3.39	3.47	<b>-1.05</b>	3.22	3.54	<b>-1.25</b>
Dystonin	Dst	4.79	4.75	<b>1.02</b>	3.12	3.44	<b>-1.25</b>
Protamine 1	Prm1	N/A	N/A	N/A	13.23	13.57	<b>-1.26</b>
Retinoblastoma-like 2	Rbl2	6.52	6.78	<b>-1.19</b>	5.31	5.64	<b>-1.26</b>
Growth arrest and DNA-damage-inducible 45 alpha	Gadd45a	6.55	5.96	<b>1.50*</b>	5.06	5.42	<b>-1.28</b>
Cyclin-dependent kinase 2	Cdk2	4.61	5.06	<b>-1.36</b>	3.62	4.01	<b>-1.31</b>
Caspase 3	Casp3	4.88	5.05	<b>-1.12</b>	4.79	5.20	<b>-1.32</b>
E2F transcription factor 3	E2f3	6.44	6.56	<b>-1.08</b>	5.85	6.30	<b>-1.36</b>
Src homology 2 domain-containing transforming protein C1	Shc1	2.93	2.88	<b>1.03</b>	3.85	4.30	<b>-1.36</b>
Stratifin	Sfn	7.34	6.98	<b>1.28</b>	8.39	8.85	<b>-1.37</b>
Cyclin E1	Ccne1	6.99	6.98	<b>1.00</b>	5.01	5.47	<b>-1.38</b>

Proteasome (prosome, macropain) assembly chaperone 2	Psmg2	4.83	5.23	<b>-1.32</b>	3.07	3.56	<b>-1.4</b>
E2F transcription factor 1	E2f1	6.53	6.71	<b>-1.12</b>	5.48	5.98	<b>-1.41</b>
CDC28 protein kinase 1b	Cks1b	2.16	2.09	<b>1.04</b>	3.01	3.56	<b>-1.46</b>
Cyclin-dependent kinase inhibitor 1B	Cdkn1b	5.93	5.92	<b>1.00</b>	3.79	4.36	<b>-1.48</b>
S-phase kinase-associated protein 2 (p45)	Skp2	5.60	6.07	<b>-1.37</b>	5.42	6.00	<b>-1.49</b>
Ataxia telangiectasia mutated homolog (human)	Atm	5.42	6.23	<b>-1.75</b>	5.56	6.14	<b>-1.50</b>
Meiotic recombination 11 homolog A ( <i>S. cerevisiae</i> )	Mre11a	5.78	5.71	<b>1.04</b>	5.10	5.68	<b>-1.50</b>
Hus1 homolog ( <i>S. pombe</i> )	Hus1	5.41	5.58	<b>-1.11</b>	6.29	6.94	<b>-1.57</b>
Calcium/calmodulin-dependent protein kinase II, beta	Camk2b	10.02	9.90	<b>1.08</b>	11.89	12.55	<b>-1.58</b>
Cyclin A2	Ccna2	3.89	4.09	<b>-1.15</b>	3.55	4.25	<b>-1.62</b>
Cyclin B2	Ccnb2	6.37	6.39	<b>-1.01</b>	4.10	4.91	<b>-1.74</b>
Minichromosome maintenance deficient 4 homolog ( <i>S. cerevisiae</i> )	Mcm4	2.34	2.54	<b>-1.14</b>	2.32	3.18	<b>-1.82</b>
E2F transcription factor 2	E2f2	N/A	N/A	N/A	11.09	12.32	<b>-2.35</b>
Cyclin A1	Ccna1	N/A	N/A	N/A	N/A	N/A	N/A
Schlafen 1	Slfn1	N/A	N/A	N/A	N/A	N/A	N/A

**Online Table II:** Pathway finder focused RT-PCR gene array in CSP cells treated with Vehicle or Wnt3a-CM.

Pathway finder RT-PCR array					
Description	Gene #	Gene Symbol	$\Delta$ Ct		Fold change
			Vehicle	Wnt3a-CM	
Insulin-like growth factor binding protein 3	31	Igfbp3	10.01	5.08	43.44*
Wingless-related MMTV integration site 2	57	Wnt2	10.1	6.55	13.94*
Fas (TNF receptor superfamily member 6)	20	Fas	8.08	5.15	10.14*
Transcription factor 7, T-cell specific	49	Tcf7	8.47	5.55	9.81*
Cyclin-dependent kinase inhibitor 2A (p16)	15	Cdkn2a	3.18	0.19	9.11*
Lymphoid enhancer binding factor 1	37	Lef1	8.02	4.97	8.52*
Prostate transmembrane protein, androgen induced 1	52	Tmepai	7.18	4.49	6.88*
Etoposide induced 2.4 mRNA	19	Ei24	4.21	3.36	1.92*
Heat shock protein 1	29	Hspb1	0.26	-0.63	1.92*
Cyclin-dependent kinase inhibitor 2B (p15, inhibits CDK4)	16	Cdkn2b	5.94	2.46	12.33
Intercellular adhesion molecule 1	30	Icam1	9.85	6.24	12.17
Fatty acid synthase	21	Fasn	9.41	7.32	9.91
FBJ osteosarcoma oncogene	23	Fos	9.12	7.07	9.83
Bone morphogenetic protein 4	8	Bmp4	8.79	7.06	9.73
Prostaglandin-endoperoxide synthase 2	46	Ptgs2	6.54	4.43	9.42
Chemokine (C-C motif) ligand 2	10	Ccl2	6.9	6.87	8.74
Baculoviral IAP repeat-containing 5	7	Birc5	6.33	7.85	8.61
Myelocytomatosis oncogene	39	Myc	6.21	6.01	6.43
Baculoviral IAP repeat-containing 2	5	Birc2	7.92	6.38	6.28
B-cell leukemia/lymphoma 2	3	Bcl2	7.31	6.31	6.09
WNT1 inducible signaling pathway protein 1	56	Wisp1	4.96	2.87	5.90
Nuclear receptor interacting protein 1	42	Nrip1	7.93	6.37	4.71
Transformed mouse 3T3 cell double minute 2	38	Mdm2	4.5	2.82	3.45
Retinol binding protein 1, cellular	47	Rbp1	2.34	1.5	3.41
Telomerase reverse transcriptase	50	Tert	8.16	6.66	3.34
Cyclin-dependent kinase inhibitor 1A (P21)	13	Cdkn1a	0.88	-0.23	3.08
Baculoviral IAP repeat-containing 3	6	Birc3	6.56	5.47	2.96
Breast cancer 1	9	Brca1	6.82	7.74	2.85
Patched homolog 1	45	Ptch1	6.35	4.98	2.84
Homeo box A1	27	Hoxa1	7.48	6.32	2.77
Jun oncogene	36	Jun	5.65	4.6	2.76
TRAF family member-associated Nf-kappa B activator	48	Tank	5.97	5.66	2.75
Peroxisome proliferator activated receptor gamma	44	Pparg	6.8	6.29	2.41



Inhibitor of kappaB kinase beta	33	Ikbbk	6.73	5.97	<b>2.36</b>
Transferrin receptor	51	Tfrc	5.58	5.44	<b>2.34</b>
Cyclin-dependent kinase 2	12	Cdk2	5.53	5.79	<b>2.05</b>
Early growth response 1	18	Egr1	5.37	6.19	<b>1.88</b>
Hexokinase 2	26	Hk2	4.76	4.2	<b>1.55</b>
Bcl2-associated X protein	2	Bax	1.16	0.58	<b>1.53</b>
Heat shock factor 1	28	Hsf1	4.37	3.84	<b>1.52</b>
Ngfi-A binding protein 2	40	Nab2	5.53	5.36	<b>1.49</b>
Vascular cell adhesion molecule 1	54	Vcam1	5.27	5.67	<b>1.49</b>
Nuclear factor of kappa light polypeptide gene enhancer in B-cells inhibitor, alpha	41	Nfkbia	4.97	4.48	<b>1.44</b>
Growth arrest and DNA-damage-inducible 45 alpha	24	Gadd45a	4.69	4.36	<b>1.43</b>
Insulin-like growth factor binding protein 4	32	Igfbp4	2.75	2.27	<b>1.43</b>
Interferon regulatory factor 1	35	Irf1	5.86	5.4	<b>1.43</b>
Cyclin-dependent kinase inhibitor 1B	14	Cdkn1b	6.77	7.02	<b>1.33</b>
Bcl2-like 1	4	Bcl2l1	5.24	5.45	<b>1.23</b>
Glycogen synthase 1, muscle	25	Gys1	4.86	4.65	<b>1.20</b>
Vascular endothelial growth factor A	55	Vegfa	4.66	4.51	<b>1.12</b>
Ornithine decarboxylase, structural 1	43	Odc1	2.11	2.14	<b>1.05</b>
Activating transcription factor 2	1	Atf2	3.55	4.46	<b>1.04</b>
Transformation related protein 53	53	Trp53	2.48	2.48	<b>1.02</b>
Cyclin D1	11	Ccnd1	2.9	3.21	<b>1.02</b>
Interleukin 4 receptor, alpha	34	Il4ra	6.09	6.67	<b>0.73</b>
Fibronectin 1	22	<td>-1.26</td> <td>-0.41</td> <td><b>0.63</b></td>	-1.26	-0.41	<b>0.63</b>
CCAAT/enhancer binding protein (C/EBP), beta	17	Cebpb	1.68	2.55	<b>0.60</b>
Bone morphogenetic protein 2	-	Bmp2	N/A	N/A	N/A
Chemokine (C-C motif) ligand 20	-	Ccl20	N/A	N/A	N/A
CD5 antigen	-	Cd5	N/A	N/A	N/A
Cadherin 1	-	Cdh1	N/A	N/A	N/A
Colony stimulating factor 2 (granulocyte-macrophage)	-	Csf2	N/A	N/A	N/A
Chemokine (C-X-C motif) ligand 1	-	Cxcl1	N/A	N/A	N/A
Chemokine (C-X-C motif) ligand 9	-	Cxcl9	N/A	N/A	N/A
Cytochrome P450, family 19, subfamily a, polypeptide 1	-	Cyp19a1	N/A	N/A	N/A
Engrailed 1	-	En1	N/A	N/A	N/A
Fas ligand (TNF superfamily, member 6)	-	Fasl	N/A	N/A	N/A
Fibroblast growth factor 4	-	Fgf4	N/A	N/A	N/A
Forkhead box A2	-	Foxa2	N/A	N/A	N/A
Gene regulated by estrogen in breast cancer protein	-	Greb1	N/A	N/A	N/A
Hedgehog-interacting protein	-	Hhip	N/A	N/A	N/A

Interleukin 1 alpha	-	Il1a	N/A	N/A	N/A
Interleukin 2	-	Il2	N/A	N/A	N/A
Interleukin 2 receptor, alpha chain	-	Il2ra	N/A	N/A	N/A
Leptin	-	Lep	N/A	N/A	N/A
Lymphotoxin A	-	Lta	N/A	N/A	N/A
Matrix metalloproteinase 10	-	Mmp10	N/A	N/A	N/A
Matrix metalloproteinase 7	-	Mmp7	N/A	N/A	N/A
NLR family, apoptosis inhibitory protein 1	-	Naip1	N/A	N/A	N/A
Nitric oxide synthase 2, inducible	-	Nos2	N/A	N/A	N/A
Selectin, endothelial cell	-	Sele	N/A	N/A	N/A
Selectin, platelet	-	Selp	N/A	N/A	N/A
Tumor necrosis factor	-	Tnf	N/A	N/A	N/A
Wingless-related MMTV integration site 1	-	Wnt1	N/A	N/A	N/A

**Online Table III:** Cell cycle-focused RT-PCR gene-arrays in CSP cells treated with Vehicle or Wnt3a-CM (48hours) and CSP cells infected with Mock or IGFBP3 o/e lentiviruses.

Cell cycle RT-PCR array						
Symbol	Wnt3a-CM treatment (48 hours)			IGFBP3 o/e		
	AVG $\Delta$ Ct		Fold change	AVG $\Delta$ Ct		Fold change
	Vehicle	Wnt3a-CM	Wnt3a/ Vehicle	Mock	IGFBP3 o/e	IGFBP3-o/e / Mock
Itgb1	-0.14	-1.36	2.33	-1.32	-1.63	1.24
Cdkn2a	2.52	1.49	2.04	1.14	0.49	1.56
Cdkn1a	1.6	1.23	1.3	0.57	-0.01	1.49
Pmp22	1.94	1.63	1.24	0.83	0.39	1.35
Ccnd1	2.49	2.23	1.20	0.95	0.7	1.19
Mdm2	1.65	1.39	1.20	0.88	0.76	1.09
Ddit3	4.82	4.61	1.16	2.9	2.75	1.11
Ak1	2.82	2.68	1.10	1.21	0.79	1.33
Notch2	5.23	5.29	-1.04	4.23	4.67	-1.36
Macf1	3.01	3.12	-1.07	2.22	2.27	-1.04
Rad17	4.81	4.99	-1.13	4.1	4.36	-1.2
Taf10	1.31	1.53	-1.16	0.57	0.85	-1.22
Sesn2	5.57	5.8	-1.17	4.25	4.27	-1.01
Ran	-1.58	-1.33	-1.19	-1.45	-1.06	-1.31
Cdk5rap1	7.76	8.03	-1.20	6.79	6.84	-1.04
E2f4	3.96	4.25	-1.22	3.14	3.41	-1.21
Pes1	2.2	2.5	-1.23	2.01	2.29	-1.22
Dnajc2	3.22	3.54	-1.25	2.74	3.09	-1.28
Rbl2	5.31	5.64	-1.26	4.55	5.42	-1.83
Cdk2	3.62	4.01	-1.31	3.83	4	-1.12
E2f3	5.85	6.3	-1.36	5.3	5.33	-1.02
Shc1	3.85	4.3	-1.36	2.63	2.76	-1.10
Sfn	8.39	8.85	-1.37	7.06	7.1	-1.03
Ccne1	5.01	5.47	-1.38	5.11	5.24	-1.09
Psmg2	3.07	3.56	-1.40	3.13	3.24	-1.08
E2f1	5.48	5.98	-1.41	4.57	4.76	-1.14
Ppm1d	4.24	4.74	-1.41	3.76	4.13	-1.29
Smc1a	3.99	4.48	-1.41	3.31	3.79	-1.40
Npm2	9.46	9.98	-1.43	8.65	8.75	-1.07
Cdc25a	4.36	4.88	-1.44	3.68	3.99	-1.25

Cks1b	3.01	3.56	-1.46	2.58	3.07	-1.41
Cdkn1b	3.79	4.36	-1.48	2.5	3.11	-1.52
Tfdp1	1.04	1.6	-1.48	1.08	1.42	-1.27
Skp2	5.42	6	-1.49	6.31	6.77	-1.37
Atm	5.56	6.14	-1.50	4.83	5.25	-1.34
Mre11a	5.1	5.68	-1.50	5.87	5.95	-1.06
Stag1	4.78	5.39	-1.52	3.86	4.37	-1.43
Terf1	4.71	5.34	-1.54	4.7	5.29	-1.51
Ccnb1	3.17	3.8	-1.55	3.11	4.38	-2.42
Hus1	6.29	6.94	-1.57	6.08	6.76	-1.60
Pcna	0.92	1.57	-1.57	1.33	2.25	-1.89
Ccna2	3.55	4.25	-1.62	2.79	4.22	-2.69
Ppp3ca	4.08	4.77	-1.62	2.86	3.16	-1.23
Rad21	1.95	2.65	-1.62	1.4	2.05	-1.57
Cdk4	1.2	1.91	-1.63	0.63	0.87	-1.18
Inha	7.77	8.47	-1.63	6.97	7.05	-1.06
Mtbp	5.13	5.84	-1.63	4.99	5.51	-1.43
Mcm3	2.86	3.57	-1.64	3.13	3.98	-1.80
Msh2	3.8	4.54	-1.66	3.71	4.12	-1.33
Chek1	5.48	6.22	-1.67	5.8	6.76	-1.95
Rad9	5.19	5.97	-1.72	4.73	5.23	-1.41
Nek2	4.28	5.07	-1.73	4.87	6.22	-2.55
Ccnb2	4.1	4.91	-1.74	4.1	5.13	-2.04
Rad51	4.99	5.81	-1.77	5.45	6.73	-2.42
Mad2l1	3.28	4.12	-1.79	3.27	4.4	-2.19
Trp53	1.83	2.68	-1.81	1.85	2.64	-1.72
Mcm4	2.32	3.18	-1.82	2.77	3.39	-1.54
Rbl1	5.69	6.57	-1.85	5.21	6.09	-1.85
Brca2	6.67	7.7	-2.04	5.97	6.64	-1.59
Wee1	5.24	6.27	-2.04	5.58	5.94	-1.28
Brca1	5.58	6.62	-2.06	5.7	7.24	-2.91
Ccnf	3.71	4.76	-2.06	3.47	4.78	-2.49
Mcm2	2.75	3.81	-2.07	3.15	4.42	-2.42
Mki67	2.94	4.07	-2.19	1.75	3.49	-3.34
E2f2	11.09	12.32	-2.35	11.35	11.75	-1.32
Trp63	10.58	13.4	-7.09	11.7	11.79	-1.06
Ppp2r3a	10.09	9.92	1.12	8.83	9.05	-1.17
Camk2a	9.14	9.14	-1.00	8.09	6.95	2.2
Pkd1	3.74	3.76	-1.01	2.73	2.43	1.23
Apbb1	8.76	8.87	-1.08	6.27	6.22	1.04
Ccnc	7.3	7.44	-1.10	5.99	5.82	1.13

Tsg101	7.03	7.17	<b>-1.10</b>	6.54	6.52	<b>1.02</b>
Nfatc1	4.46	4.63	<b>-1.12</b>	2.93	2.91	<b>1.01</b>
Sumo1	2.1	2.28	<b>-1.13</b>	1.76	1.61	<b>1.11</b>
Gpr132	12.38	12.6	<b>-1.17</b>	11.95	11.79	<b>1.12</b>
Abl1	9.49	9.76	<b>-1.21</b>	8.13	7.72	<b>1.33</b>
Dst	3.12	3.44	<b>-1.25</b>	2.2	2.07	<b>1.09</b>
Prm1	13.23	13.57	<b>-1.26</b>	12.07	11.79	<b>1.21</b>
Gadd45a	5.06	5.42	<b>-1.28</b>	4.41	3.51	<b>1.86</b>
Casp3	4.79	5.2	<b>-1.32</b>	3.98	3.86	<b>1.09</b>
Ccna1	13.27	13.75	<b>-1.39</b>	12.07	11.79	<b>1.21</b>
Slfn1	13.27	13.75	<b>-1.39</b>	12.07	11.79	<b>1.21</b>
Camk2b	11.89	12.55	<b>-1.58</b>	10.26	9.78	<b>1.40</b>
Myb	12.28	13.25	<b>-1.96</b>	11.85	11.79	<b>1.04</b>



Online Table IV: Cell cycle-focused RT-PCR gene arrays in CSP cells infected with sh-Scramble and sh-IGFBP3 lentiviruses and treated with Vehicle or Wnt3a-CM (5 days).

Cell cycle RT-PCR array							
Description	Symbol	Sh-Scramble			Sh-IGFBP3		
		( $\Delta$ Ct)		Fold change	( $\Delta$ Ct)		Fold change
		Vehicle	Wnt3a-CM		Vehicle	Wnt3a-CM	
Minichromosome maintenance deficient 3 ( <i>S. cerevisiae</i> )	Mcm3	4.79	1.60	-9.18	1.58	2.00	1.33
Cyclin B1	Ccnb1	6.55	3.65	-7.51	1.93	3.32	2.61
Proliferating cell nuclear antigen	Pcna	4.66	1.78	-7.40	1.52	1.97	1.36
Cyclin-dependent kinase 2	Cdk2	7.43	4.56	-7.35	4.20	4.64	1.35
Cyclin A2	Ccna2	5.21	2.69	-5.77	1.12	2.21	2.12
Cyclin B2	Ccnb2	8.64	6.26	-5.23	4.61	5.02	1.33
Breast cancer 1	Brca1	7.76	5.59	-4.53	4.59	5.71	2.17
Minichromosome maintenance deficient 4 homolog ( <i>S. cerevisiae</i> )	Mcm4	4.64	2.49	-4.46	2.06	2.25	1.14
MAD2 mitotic arrest deficient-like 1 (yeast)	Mad2l1	5.72	3.60	-4.37	3.05	3.12	1.05
E2F transcription factor 3	E2f3	7.48	5.55	-3.83	5.21	5.96	1.68
Antigen identified by monoclonal antibody Ki 67	Mki67	3.21	1.36	-3.63	1.25	1.50	1.19
Meiotic recombination 11 homolog A ( <i>S. cerevisiae</i> )	Mre11a	8.64	6.82	-3.55	5.53	6.98	2.72
Breast cancer 2	Brca2	7.38	5.58	-3.50	3.52	4.55	2.04
Minichromosome maintenance deficient 2 mitotin ( <i>S. cerevisiae</i> )	Mcm2	4.85	3.17	-3.22	2.49	2.89	1.32
RAN, member RAS oncogene family	Ran	0.93	-0.63	-2.96	-1.10	-0.94	1.11
Cyclin-dependent kinase inhibitor 1B	Cdkn1b	5.02	3.48	-2.92	3.11	3.24	1.09
Checkpoint kinase 1 homolog ( <i>S. pombe</i> )	Chek1	6.89	5.43	-2.77	5.45	5.60	1.11
CDC28 protein kinase 1b	Cks1b	4.51	3.05	-2.77	2.65	2.78	1.09
Retinoblastoma-like 1 (p107)	Rbl1	6.76	5.32	-2.73	5.50	5.60	1.07
S-phase kinase-associated protein 2 (p45)	Skp2	8.54	7.10	-2.73	6.01	7.48	2.76
WEE 1 homolog 1 ( <i>S. pombe</i> )	Wee1	7.44	6.04	-2.65	5.08	6.36	2.42
Caspase 3	Casp3	6.79	5.50	-2.46	4.30	5.99	3.22
SMT3 suppressor of mif two 3 homolog 1 (yeast)	Sumo1	4.33	3.06	-2.43	3.35	3.37	1.01
Cyclin F	Ccnf	4.41	3.17	-2.38	2.59	2.63	1.03

Mdm2, transformed 3T3 cell double minute p53 binding protein	Mtpb	5.70	4.50	-2.31	3.53	4.37	1.79
Retinoblastoma-like 2	Rbl2	8.63	7.45	-2.28	6.41	7.28	1.82
MutS homolog 2 (E. coli)	Msh2	4.31	3.16	-2.23	2.30	2.65	1.27
Pescadillo homolog 1, containing BRCT domain (zebrafish)	Pes1	1.99	0.86	-2.20	1.12	0.47	-1.57
Telomeric repeat binding factor 1	Terf1	5.49	4.38	-2.17	4.98	5.02	1.03
Ataxia telangiectasia mutated homolog (human)	Atm	5.78	4.70	-2.13	3.43	4.60	2.24
Tumor susceptibility gene 101	Tsg101	8.42	7.38	-2.07	5.42	6.43	2.01
C-abl oncogene 1, receptor tyrosine kinase	Abl1	7.41	6.60	-1.76	7.40	7.44	1.03
RAD51 homolog (S. cerevisiae)	Rad51	8.64	7.95	-1.62	7.17	7.68	1.42
Protein phosphatase 1D magnesium-dependent, delta isoform	Ppm1d	4.03	3.37	-1.59	2.86	2.93	1.05
RAD21 homolog (S. pombe)	Rad21	2.14	1.56	-1.50	1.58	1.21	-1.30
Transformation related protein 53	Trp53	1.88	1.34	-1.46	1.27	0.98	-1.23
Src homology 2 domain-containing transforming protein C1	Shc1	3.87	3.42	-1.37	2.41	2.92	1.42
NIMA (never in mitosis gene a) related expressed kinase 2	Nek2	4.80	4.36	-1.36	3.33	3.34	1.00
Cyclin C	Ccnc	8.64	8.25	-1.32	7.27	7.13	-1.11
Nucleophosmin/nucleoplasm in 2	Npm2	8.64	8.27	-1.30	8.47	8.03	-1.36
Protein phosphatase 3, catalytic subunit, alpha isoform	Ppp3ca	4.40	4.04	-1.29	2.79	2.66	-1.10
Structural maintenance of chromosomes 1A	Smc1a	4.22	3.91	-1.25	3.66	3.30	-1.29
Transcription factor Dp 1	Tfdp1	2.08	1.77	-1.25	1.04	1.15	1.08
Stromal antigen 1	Stag1	4.92	4.64	-1.22	4.49	4.20	-1.23
Cyclin E1	Ccne1	4.33	4.07	-1.20	3.28	4.89	3.04
E2F transcription factor 4	E2f4	2.94	2.70	-1.19	2.15	2.35	1.15
E2F transcription factor 1	E2f1	5.18	4.95	-1.18	3.82	4.28	1.37
RAD17 homolog (S. pombe)	Rad17	4.83	4.60	-1.18	4.48	4.40	-1.06
Adenylate kinase 1	Ak1	2.70	2.49	-1.16	1.27	2.16	1.85
RAD9 homolog (S. pombe)	Rad9	4.49	4.33	-1.12	4.37	3.99	-1.31
Hus1 homolog (S. pombe)	Hus1	5.87	5.73	-1.11	4.81	5.23	1.33
Growth arrest and DNA damage-inducible 45 alpha	Gadd45a	4.31	4.19	-1.09	3.45	4.07	1.53
Transformed mouse 3T3 cell double minute 2	Mdm2	2.92	2.85	-1.06	1.47	1.94	1.38
Proteasome (prosome, macropain) assembly chaperone 2	Psmg2	3.41	3.38	-1.03	2.73	3.04	1.24

Integrin beta 1 (fibronectin receptor beta)	Itgb1	-4.12	-1.26	7.22	-2.38	-1.51	1.82
Polycystic kidney disease 1 homolog	Pkd1	1.33	2.92	2.99	3.10	2.99	-1.08
DNA-damage inducible transcript 3	Ddit3	1.64	3.22	2.97	3.24	2.55	-1.62
Dystonin	Dst	0.26	1.84	2.97	1.46	0.73	-1.66
Sestrin 2	Sesn2	2.81	4.30	2.79	3.78	4.01	1.17
Microtubule-actin crosslinking factor 1	Macf1	0.44	1.75	2.47	1.36	1.32	-1.03
Cyclin D1	Ccnd1	1.46	2.70	2.35	1.66	2.58	1.89
Cyclin-dependent kinase inhibitor 1A (P21)	Cdkn1a	-0.79	0.45	2.35	0.07	0.24	1.12
Cyclin-dependent kinase inhibitor 2A	Cdkn2a	0.62	1.81	2.27	1.02	1.57	1.46
Calcium/calmodulin-dependent protein kinase II alpha	Camk2a	5.28	6.23	1.92	5.49	7.52	4.07
CDK5 regulatory subunit associated protein 1	Cdk5rap1	5.73	6.49	1.68	5.84	6.16	1.24
Stratifin	Sfn	6.24	6.99	1.67	6.26	7.06	1.74
Notch gene homolog 2 (Drosophila)	Notch2	3.58	4.27	1.60	3.73	3.74	1.00
Nuclear factor of activated T-cells, cytoplasmic, calcineurin-dependent 1	Nfatc1	3.94	4.45	1.42	3.85	3.41	-1.36
DnaJ (Hsp40) homolog, subfamily C, member 2	Dnajc2	2.04	2.44	1.31	1.89	1.77	-1.09
Amyloid beta (A4) precursor protein-binding, family B, member 1	Apbb1	5.56	5.93	1.29	5.68	5.79	1.08
Cyclin-dependent kinase 4	Cdk4	0.74	1.03	1.22	0.86	0.80	-1.05
Peripheral myelin protein 22	Pmp22	1.53	1.79	1.19	2.13	2.22	1.06
Inhibin alpha	Inha	6.58	6.81	1.17	7.22	6.23	-1.99
TAF10 RNA polymerase II, TATA box binding protein (TBP)-associated factor	Taf10	0.11	0.22	1.07	0.10	-0.58	-1.61
Cell division cycle 25 homolog A (S. pombe)	Cdc25a	3.27	3.37	1.07	3.31	3.45	1.10
Calcium/calmodulin-dependent protein kinase II, beta	Camk2b	N/A	N/A	N/A	N/A	N/A	N/A
Cyclin A1	Ccna1	N/A	N/A	N/A	N/A	N/A	N/A
E2F transcription factor 2	E2f2	N/A	N/A	N/A	N/A	N/A	N/A
G protein-coupled receptor 132	Gpr132	N/A	N/A	N/A	N/A	N/A	N/A
Myeloblastosis oncogene	Myb	N/A	N/A	N/A	N/A	N/A	N/A
Protein phosphatase 2 (formerly 2A), regulatory subunit B", alpha	Ppp2r3a	N/A	N/A	N/A	N/A	N/A	N/A
Protamine 1	Prm1	N/A	N/A	N/A	N/A	N/A	N/A

Schlafen 1	Slfn1	N/A	N/A	N/A	N/A	N/A	N/A
Transformation related protein 63	Trp63	N/A	N/A	N/A	N/A	N/A	N/A

**Online Table V:** Wnt signaling focused RT-PCR gene array in freshly isolated CSP cells from sham and 1 day post-MI mice.

<b>Wnt signaling RT-PCR array</b>				
<b>Description</b>	<b>Symbol</b>	<b>Day 1 post-MI (<math>\Delta</math>Ct)</b>		
		<b>Sham</b>	<b>post-MI</b>	<b>Fold change</b>
Casein kinase 1, delta	Csnk1d	2.59	3.22	<b>-1.55*</b>
Jun oncogene	Jun	-2.42	-2.38	<b>-1.02</b>
F-box and WD-40 domain protein 11	Fbxw11	5.69	5.72	<b>-1.02</b>
Secreted frizzled-related protein 4	Sfrp4	5.67	5.72	<b>-1.03</b>
Amino-terminal enhancer of split	Aes	3.42	3.48	<b>-1.04</b>
Cyclin D3	Ccnd3	2.18	2.24	<b>-1.04</b>
Transducin-like enhancer of split 1, homolog of Drosophila E(spl)	Tle1	4.56	4.69	<b>-1.09</b>
Casein kinase 1, alpha 1	Csnk1a1	2.04	2.18	<b>-1.10</b>
Frizzled homolog 1 (Drosophila)	Fzd1	2.86	3.01	<b>-1.10</b>
Low density lipoprotein receptor-related protein 6	Lrp6	2.76	2.92	<b>-1.11</b>
Protein phosphatase 2a, regulatory subunit A (PR 65)	Ppp2r1a	1.53	1.71	<b>-1.12</b>
Casein kinase 2, alpha 1 polypeptide	Csnk2a1	2.48	2.64	<b>-1.12</b>
Protein phosphatase 2 (formerly 2A), catalytic subunit, alpha isoform	Ppp2ca	1.39	1.58	<b>-1.14</b>
Dishevelled 2, dsh homolog (Drosophila)	Dvl2	4.31	4.52	<b>-1.15</b>
Kringle containing transmembrane protein 1	Kremen1	2.43	2.67	<b>-1.17</b>
C-terminal binding protein 1	Ctbp1	1.62	1.90	<b>-1.21</b>
Wingless-related MMTV integration site 4	Wnt4	5.44	5.72	<b>-1.21</b>
Secreted frizzled-related protein 2	Sfrp2	2.07	2.37	<b>-1.22</b>
Ras homolog gene family, member U	Rhou	4.83	5.14	<b>-1.24</b>
Secreted frizzled-related protein 1	Sfrp1	3.66	4.00	<b>-1.26</b>
Fos-like antigen 1	Fosl1	2.72	3.08	<b>-1.27</b>
Dishevelled, dsh homolog 1 (Drosophila)	Dvl1	5.01	5.37	<b>-1.28</b>
Catenin (cadherin associated protein), beta 1	Ctnnb1	0.37	0.78	<b>-1.33</b>
SUMO/sentrin specific peptidase 2	Senp2	5.31	5.72	<b>-1.33</b>
Low density lipoprotein receptor-related protein 5	Lrp5	2.51	2.97	<b>-1.37</b>
Frizzled homolog 7 (Drosophila)	Fzd7	3.80	4.26	<b>-1.37</b>



Frizzled homolog 2 (Drosophila)	Fzd2	5.67	5.20	<b>1.38</b>
Transcription factor 3	Tcf3	4.69	5.17	<b>-1.39</b>
Frizzled homolog 4 (Drosophila)	Fzd4	3.50	3.98	<b>-1.39</b>
C-terminal binding protein 2	Ctbp2	1.93	2.41	<b>-1.39</b>
Protein phosphatase 2d, regulatory subunit B (B56)	Ppp2r5d	3.18	3.70	<b>-1.43</b>
Axin 1	Axin1	3.51	4.13	<b>-1.53</b>
Catenin beta interacting protein 1	Ctnnbip1	4.56	5.22	<b>-1.57</b>
WNT1 inducible signaling pathway protein 1	Wisp1	5.02	5.72	<b>-1.63</b>
Frizzled homolog 5 (Drosophila)	Fzd5	4.04	4.78	<b>-1.67</b>
E1A binding protein p300	Ep300	4.61	5.37	<b>-1.68</b>
Cyclin D1	Ccnd1	4.52	5.27	<b>-1.68</b>
Frizzled homolog 6 (Drosophila)	Fzd6	4.48	5.28	<b>-1.73</b>
Naked cuticle 1 homolog (Drosophila)	Nkd1	3.89	4.87	<b>-1.98</b>
Adenomatous polyposis coli	Apc	4.03	5.24	<b>-2.30</b>
Solute carrier family 9 (sodium/hydrogen exchanger), member 3 regulator 1	Slc9a3r1	5.53	5.53	<b>1.00</b>
Myelocytomatosis oncogene	Myc	2.90	2.89	<b>1.00</b>
F-box and WD-40 domain protein 2	Fbxw2	3.22	3.20	<b>1.01</b>
B-cell CLL/lymphoma 9	Bcl9	5.76	5.72	<b>1.02</b>
Lymphoid enhancer binding factor 1	Lef1	5.76	5.72	<b>1.02</b>
Frizzled homolog 8 (Drosophila)	Fzd8	5.77	5.72	<b>1.03</b>
Cyclin D2	Ccnd2	2.72	2.65	<b>1.05</b>
SRY-box containing gene 17	Sox17	3.75	3.66	<b>1.06</b>
Wingless-type MMTV integration site 9A	Wnt9a	5.81	5.72	<b>1.06</b>
Pygopus 1	Pygo1	5.69	5.59	<b>1.07</b>
Wingless-related MMTV integration site 11	Wnt11	4.33	4.23	<b>1.07</b>
Dishevelled associated activator of morphogenesis 1	Daam1	3.57	3.45	<b>1.08</b>
Wingless related MMTV integration site 2b	Wnt2b	5.15	5.00	<b>1.10</b>
F-box and WD-40 domain protein 4	Fbxw4	5.87	5.72	<b>1.10</b>
Frizzled homolog 3 (Drosophila)	Fzd3	5.89	5.72	<b>1.12</b>
DIX domain containing 1	Dixdc1	5.61	5.40	<b>1.15</b>
Glycogen synthase kinase 3 beta	Gsk3b	5.97	5.72	<b>1.18</b>
Beta-transducin repeat containing protein	Btrc	6.03	5.72	<b>1.23</b>
Frizzled-related protein	Frzb	2.15	1.81	<b>1.26</b>
Porcupine homolog (Drosophila)	Porcn	6.03	5.64	<b>1.30</b>
Wingless-related MMTV integration site 5B	Wnt5b	5.56	5.16	<b>1.32</b>

Wingless-related MMTV integration site 5A	Wnt5a	6.15	5.72	<b>1.34</b>
Transcription factor 7, T-cell specific	Tcf7	5.86	5.21	<b>1.57</b>
Follicle stimulating hormone beta	Fshb	6.17	5.51	<b>1.58</b>
Wingless-related MMTV integration site 16	Wnt16	6.17	5.44	<b>1.65</b>
Wnt inhibitory factor 1	Wif1	4.42	3.08	<b>2.52</b>
Dickkopf homolog 1 ( <i>Xenopus laevis</i> )	Dkk1	N/A	N/A	N/A
Fibroblast growth factor 4	Fgf4	N/A	N/A	N/A
Forkhead box N1	Foxn1	N/A	N/A	N/A
Frequently rearranged in advanced T-cell lymphomas	Frat1	N/A	N/A	N/A
Nemo like kinase	Nlk	N/A	N/A	N/A
Paired-like homeodomain transcription factor 2	Pitx2	N/A	N/A	N/A
Brachyury	T	N/A	N/A	N/A
Transducin-like enhancer of split 2, homolog of <i>Drosophila</i> E(spl)	Tle2	N/A	N/A	N/A
Wingless-related MMTV integration site 1	Wnt1	N/A	N/A	N/A
Wingless related MMTV integration site 10a	Wnt10a	N/A	N/A	N/A
Wingless-related MMTV integration site 2	Wnt2	N/A	N/A	N/A
Wingless-related MMTV integration site 3	Wnt3	N/A	N/A	N/A
Wingless-related MMTV integration site 3A	Wnt3a	N/A	N/A	N/A
Wingless-related MMTV integration site 6	Wnt6	N/A	N/A	N/A
Wingless-related MMTV integration site 7A	Wnt7a	N/A	N/A	N/A
Wingless-related MMTV integration site 7B	Wnt7b	N/A	N/A	N/A
Wingless-related MMTV integration site 8A	Wnt8a	N/A	N/A	N/A
Wingless related MMTV integration site 8b	Wnt8b	N/A	N/A	N/A

**Online Table VI:** Wnt signaling focused RT-PCR gene array in freshly isolated CSP cells from sham and 3 days post-MI mice.

<b>Wnt signaling RT-PCR array</b>				
<b>Description</b>	<b>Symbol</b>	<b>Day 3 post-MI (<math>\Delta</math>Ct)</b>		
		<b>Sham</b>	<b>post-MI</b>	<b>Fold change</b>
Frizzled homolog 5 (Drosophila)	Fzd5	4.03	5.03	<b>-1.99*</b>
Adenomatosis polyposis coli	Apc	4.03	5.07	<b>-2.07*</b>
Dishevelled 2, dsh homolog (Drosophila)	Dvl2	4.30	5.47	<b>-2.25*</b>
Amino-terminal enhancer of split	Aes	3.42	4.75	<b>-2.52*</b>
Transcription factor 3	Tcf3	4.68	6.09	<b>-2.65*</b>
E1A binding protein p300	Ep300	4.61	6.02	<b>-2.66*</b>
Secreted frizzled-related protein 4	Sfrp4	5.66	7.29	<b>-3.00*</b>
Frizzled homolog 6 (Drosophila)	Fzd6	4.48	6.44	<b>-3.89*</b>
Ras homolog gene family, member U	Rhou	4.83	4.84	<b>-1.00</b>
Frizzled-related protein	Frzb	2.15	2.18	<b>-1.01</b>
Frizzled homolog 1 (Drosophila)	Fzd1	2.86	2.91	<b>-1.03</b>
Casein kinase 1, alpha 1	Csnk1a1	2.04	2.23	<b>-1.13</b>
Wingless-related MMTV integration site 11	Wnt11	4.33	4.52	<b>-1.14</b>
Transducin-like enhancer of split 1, homolog of Drosophila E(spl)	Tle1	4.56	4.79	<b>-1.16</b>
Myelocytomatosis oncogene	Myc	2.90	3.16	<b>-1.19</b>
Secreted frizzled-related protein 1	Sfrp1	3.66	3.96	<b>-1.22</b>
Cyclin D1	Ccnd1	4.52	4.85	<b>-1.25</b>
Protein phosphatase 2a, regulatory subunit A (PR 65)	Ppp2r1a	1.53	1.91	<b>-1.29</b>
F-box and WD-40 domain protein 2	Fbxw2	3.22	3.61	<b>-1.30</b>
Wnt inhibitory factor 1	Wif1	4.42	4.85	<b>-1.34</b>
SUMO/sentrin specific peptidase 2	Senp2	5.31	5.74	<b>-1.34</b>
Fos-like antigen 1	Fosl1	2.72	3.19	<b>-1.38</b>
C-terminal binding protein 1	Ctbp1	1.62	2.10	<b>-1.39</b>
Low density lipoprotein receptor-related protein 6	Lrp6	2.76	3.26	<b>-1.40</b>
Dishevelled associated activator of morphogenesis 1	Daam1	3.57	4.12	<b>-1.45</b>
Transcription factor 7, T-cell specific	Tcf7	5.86	6.42	<b>-1.47</b>
F-box and WD-40 domain protein 11	Fbxw11	5.69	6.32	<b>-1.54</b>
Axin 1	Axin1	3.51	4.15	<b>-1.55</b>
Catenin (cadherin associated protein), beta 1	Ctnnb1	0.37	1.03	<b>-1.57</b>
Kringle containing transmembrane protein 1	Kremen1	2.43	3.13	<b>-1.61</b>

Frizzled homolog 2 (Drosophila)	Fzd2	5.67	6.36	<b>-1.61</b>
Casein kinase 1, delta	Csnk1d	2.59	3.31	<b>-1.63</b>
Solute carrier family 9 (sodium/hydrogen exchanger), member 3 regulator 1	Slc9a3r1	5.53	6.25	<b>-1.64</b>
C-terminal binding protein 2	Ctbp2	1.93	2.72	<b>-1.72</b>
Glycogen synthase kinase 3 beta	Gsk3b	5.97	6.76	<b>-1.73</b>
Wingless related MMTV integration site 2b	Wnt2b	5.15	5.94	<b>-1.73</b>
Cyclin D3	Ccnd3	2.18	2.99	<b>-1.74</b>
Wingless-related MMTV integration site 4	Wnt4	5.44	6.25	<b>-1.75</b>
Dishevelled, dsh homolog 1 (Drosophila)	Dvl1	5.01	5.82	<b>-1.75</b>
Casein kinase 2, alpha 1 polypeptide	Csnk2a1	2.48	3.30	<b>-1.76</b>
Low density lipoprotein receptor-related protein 5	Lrp5	2.51	3.34	<b>-1.77</b>
Wingless-related MMTV integration site 5A	Wnt5a	6.15	7.00	<b>-1.80</b>
Cyclin D2	Ccnd2	2.72	3.59	<b>-1.82</b>
Frizzled homolog 3 (Drosophila)	Fzd3	5.89	6.83	<b>-1.91</b>
Jun oncogene	Jun	-2.42	-1.47	<b>-1.92</b>
Porcupine homolog (Drosophila)	Porcn	6.03	7.00	<b>-1.96</b>
Frizzled homolog 8 (Drosophila)	Fzd8	5.77	6.76	<b>-1.97</b>
Frizzled homolog 7 (Drosophila)	Fzd7	3.80	4.85	<b>-2.06</b>
F-box and WD-40 domain protein 4	Fbxw4	5.87	6.95	<b>-2.11</b>
Wingless-type MMTV integration site 9A	Wnt9a	5.81	6.90	<b>-2.11</b>
Catenin beta interacting protein 1	Ctnnbip1	4.56	5.70	<b>-2.20</b>
Wingless-related MMTV integration site 5B	Wnt5b	5.56	6.71	<b>-2.21</b>
B-cell CLL/lymphoma 9	Bcl9	5.76	6.94	<b>-2.25</b>
Frizzled homolog 4 (Drosophila)	Fzd4	3.50	4.69	<b>-2.27</b>
Naked cuticle 1 homolog (Drosophila)	Nkd1	3.89	5.07	<b>-2.27</b>
DIX domain containing 1	Dixdc1	5.61	6.81	<b>-2.28</b>
Beta-transducin repeat containing protein	Btrc	6.03	7.23	<b>-2.29</b>
Lymphoid enhancer binding factor 1	Lef1	5.76	7.15	<b>-2.61</b>
Pygopus 1	Pygo1	5.69	7.16	<b>-2.76</b>
SRY-box containing gene 17	Sox17	3.75	5.44	<b>-3.23</b>
Secreted frizzled-related protein 2	Sfrp2	2.07	1.57	<b>1.41</b>
WNT1 inducible signaling pathway protein 1	Wisp1	5.02	4.71	<b>1.23</b>
Protein phosphatase 2d, regulatory subunit B (B56)	Ppp2r5d	3.18	3.03	<b>1.11</b>
Protein phosphatase 2 (formerly 2A), catalytic subunit, alpha isoform	Ppp2ca	1.39	1.27	<b>1.08</b>
Dickkopf homolog 1 (Xenopus laevis)	Dkk1	N/A	N/A	N/A
Fibroblast growth factor 4	Fgf4	N/A	N/A	N/A
Forkhead box N1	Foxn1	N/A	N/A	N/A

Frequently rearranged in advanced T-cell lymphomas	Frat1	N/A	N/A	N/A
Follicle stimulating hormone beta	Fshb	N/A	N/A	N/A
Nemo like kinase	Nlk	N/A	N/A	N/A
Paired-like homeodomain transcription factor 2	Pitx2	N/A	N/A	N/A
Brachyury	T	N/A	N/A	N/A
Transducin-like enhancer of split 2, homolog of Drosophila E(spl)	Tle2	N/A	N/A	N/A
Wingless-related MMTV integration site 1	Wnt1	N/A	N/A	N/A
Wingless related MMTV integration site 10a	Wnt10a	N/A	N/A	N/A
Wingless-related MMTV integration site 16	Wnt16	N/A	N/A	N/A
Wingless-related MMTV integration site 2	Wnt2	N/A	N/A	N/A
Wingless-related MMTV integration site 3	Wnt3	N/A	N/A	N/A
Wingless-related MMTV integration site 3A	Wnt3a	N/A	N/A	N/A
Wingless-related MMTV integration site 6	Wnt6	N/A	N/A	N/A
Wingless-related MMTV integration site 7A	Wnt7a	N/A	N/A	N/A
Wingless-related MMTV integration site 7B	Wnt7b	N/A	N/A	N/A
Wingless-related MMTV integration site 8A	Wnt8a	N/A	N/A	N/A
Wingless related MMTV integration site 8b	Wnt8b	N/A	N/A	N/A



**Online Table VII:** Wnt signaling focused RT-PCR gene array in freshly isolated CSP cells from sham and 7 days post-MI mice.

<b>Wnt signaling RT-PCR array</b>				
<b>Description</b>	<b>Symbol</b>	<b>Day 7 post-MI (<math>\Delta</math>Ct)</b>		
		<b>Sham</b>	<b>post-MI</b>	<b>Fold change</b>
Catenin (cadherin associated protein), beta 1	Ctnnb1	0.09	0.47	<b>-1.30*</b>
C-terminal binding protein 1	Ctbp1	1.73	2.36	<b>-1.54*</b>
Wnt inhibitory factor 1	Wif1	3.50	4.34	<b>-1.78*</b>
Casein kinase 1, alpha 1	Csnk1a1	1.99	2.87	<b>-1.83*</b>
Cyclin D2	Ccnd2	2.13	3.58	<b>-2.74*</b>
Amino-terminal enhancer of split	Aes	2.77	4.74	<b>-3.91*</b>
Protein phosphatase 2a, regulatory subunit A (PR 65)	Ppp2r1a	1.79	1.80	<b>-1.00</b>
Frizzled homolog 1 (Drosophila)	Fzd1	3.11	3.13	<b>-1.01</b>
Pygopus 1	Pygo1	5.13	5.17	<b>-1.02</b>
Transcription factor 3	Tcf3	4.80	4.84	<b>-1.02</b>
Casein kinase 2, alpha 1 polypeptide	Csnk2a1	2.83	2.88	<b>-1.03</b>
Solute carrier family 9 (sodium/hydrogen exchanger), member 3 regulator 1	Slc9a3r1	4.94	5.02	<b>-1.05</b>
Frizzled-related protein	Frzb	2.12	2.23	<b>-1.07</b>
Frizzled homolog 5 (Drosophila)	Fzd5	4.11	4.22	<b>-1.07</b>
Wingless-related MMTV integration site 11	Wnt11	4.53	4.66	<b>-1.09</b>
Dishevelled 2, dsh homolog (Drosophila)	Dvl2	4.16	4.31	<b>-1.10</b>
Frizzled homolog 3 (Drosophila)	Fzd3	5.09	5.34	<b>-1.18</b>
Myelocytomatosis oncogene	Myc	3.08	3.32	<b>-1.18</b>
Frizzled homolog 8 (Drosophila)	Fzd8	5.01	5.27	<b>-1.19</b>
Frizzled homolog 4 (Drosophila)	Fzd4	3.14	3.41	<b>-1.2</b>
Secreted frizzled-related protein 1	Sfrp1	3.78	4.06	<b>-1.21</b>
Secreted frizzled-related protein 4	Sfrp4	5.04	5.34	<b>-1.22</b>
Protein phosphatase 2d, regulatory subunit B (B56)	Ppp2r5d	3.04	3.37	<b>-1.24</b>
C-terminal binding protein 2	Ctbp2	1.86	2.25	<b>-1.31</b>
Casein kinase 1, delta	Csnk1d	2.82	3.26	<b>-1.35</b>
Low density lipoprotein receptor-related protein 6	Lrp6	2.57	3.01	<b>-1.35</b>
B-cell CLL/lymphoma 9	Bcl9	4.88	5.34	<b>-1.36</b>
Naked cuticle 1 homolog (Drosophila)	Nkd1	3.72	4.16	<b>-1.36</b>
F-box and WD-40 domain protein 2	Fbxw2	2.66	3.12	<b>-1.37</b>
E1A binding protein p300	Ep300	4.21	4.69	<b>-1.38</b>
SRY-box containing gene 17	Sox17	2.71	3.19	<b>-1.39</b>
Transcription factor 7, T-cell specific	Tcf7	4.37	4.85	<b>-1.39</b>
Kringle containing transmembrane protein 1	Kremen1	2.47	2.96	<b>-1.40</b>

Low density lipoprotein receptor-related protein 5	Lrp5	2.10	2.63	<b>-1.44</b>
Porcupine homolog (Drosophila)	Porcn	4.79	5.34	<b>-1.45</b>
Frizzled homolog 7 (Drosophila)	Fzd7	3.93	4.49	<b>-1.47</b>
Wingless-related MMTV integration site 5A	Wnt5a	4.72	5.29	<b>-1.48</b>
Jun oncogene	Jun	-2.87	-2.22	<b>-1.57</b>
SUMO/sentrin specific peptidase 2	Senp2	4.24	4.93	<b>-1.6</b>
Ras homolog gene family, member U	Rhou	4.11	4.80	<b>-1.61</b>
Frizzled homolog 2 (Drosophila)	Fzd2	4.63	5.34	<b>-1.62</b>
Catenin beta interacting protein 1	Ctnnbip1	3.96	4.74	<b>-1.71</b>
Cyclin D3	Ccnd3	1.33	2.12	<b>-1.72</b>
Wingless related MMTV integration site 2b	Wnt2b	4.05	4.85	<b>-1.73</b>
Adenomatosis polyposis coli	Apc	3.79	4.64	<b>-1.80</b>
Fos-like antigen 1	Fosl1	3.24	4.17	<b>-1.90</b>
Cyclin D1	Ccnd1	3.46	4.41	<b>-1.92</b>
Axin 1	Axin1	3.45	4.47	<b>-2.01</b>
Dishevelled associated activator of morphogenesis 1	Daam1	3.15	4.20	<b>-2.06</b>
Dishevelled, dsh homolog 1 (Drosophila)	Dvl1	3.91	5.06	<b>-2.21</b>
Secreted frizzled-related protein 2	Sfrp2	3.07	1.66	<b>2.66*</b>
Transducin-like enhancer of split 1, homolog of Drosophila E(spl)	Tle1	5.04	4.21	<b>1.77</b>
Wingless-related MMTV integration site 5B	Wnt5b	4.70	4.44	<b>1.19</b>
Protein phosphatase 2 (formerly 2A), catalytic subunit, alpha isoform	Ppp2ca	1.42	1.28	<b>1.09</b>
WNT1 inducible signaling pathway protein 1	Wisp1	5.13	5.01	<b>1.09</b>
Wingless-related MMTV integration site 4	Wnt4	5.13	5.00	<b>1.09</b>
Frizzled homolog 6 (Drosophila)	Fzd6	3.97	3.96	<b>1.00</b>
Glycogen synthase kinase 3 beta	Gsk3b	5.13	5.12	<b>1.00</b>
Beta-transducin repeat containing protein	Btrc	N/A	N/A	N/A
DIX domain containing 1	Dixdc1	N/A	N/A	N/A
Dickkopf homolog 1 (Xenopus laevis)	Dkk1	N/A	N/A	N/A
F-box and WD-40 domain protein 11	Fbxw11	N/A	N/A	N/A
F-box and WD-40 domain protein 4	Fbxw4	N/A	N/A	N/A
Fibroblast growth factor 4	Fgf4	N/A	N/A	N/A
Forkhead box N1	Foxn1	N/A	N/A	N/A
Frequently rearranged in advanced T-cell lymphomas	Frat1	N/A	N/A	N/A
Follicle stimulating hormone beta	Fshb	N/A	N/A	N/A
Lymphoid enhancer binding factor 1	Lef1	N/A	N/A	N/A
Nemo like kinase	Nlk	N/A	N/A	N/A
Paired-like homeodomain transcription factor 2	Pitx2	N/A	N/A	N/A
Brachyury	T	N/A	N/A	N/A

Transducin-like enhancer of split 2, homolog of Drosophila E(spl)	Tle2	N/A	N/A	N/A
Wingless-related MMTV integration site 1	Wnt1	N/A	N/A	N/A
Wingless related MMTV integration site 10a	Wnt10a	N/A	N/A	N/A
Wingless-related MMTV integration site 16	Wnt16	N/A	N/A	N/A
Wingless-related MMTV integration site 2	Wnt2	N/A	N/A	N/A
Wingless-related MMTV integration site 3	Wnt3	N/A	N/A	N/A
Wingless-related MMTV integration site 3A	Wnt3a	N/A	N/A	N/A
Wingless-related MMTV integration site 6	Wnt6	N/A	N/A	N/A
Wingless-related MMTV integration site 7A	Wnt7a	N/A	N/A	N/A
Wingless-related MMTV integration site 7B	Wnt7b	N/A	N/A	N/A
Wingless-related MMTV integration site 8A	Wnt8a	N/A	N/A	N/A
Wingless related MMTV integration site 8b	Wnt8b	N/A	N/A	N/A
Wingless-type MMTV integration site 9A	Wnt9a	N/A	N/A	N/A

**Online Table VIII:** Order of Wnt signaling relates genes on the RT-PCR array 96-well plate corresponding to Figure 4A-C. MGDC (Mouse Genomic DNA Contamination), RTC (Reverse Transcription Control) and PPC (Polymerase PCR Control) represent internal array controls and are not depicted in **Figure 4A-C**.

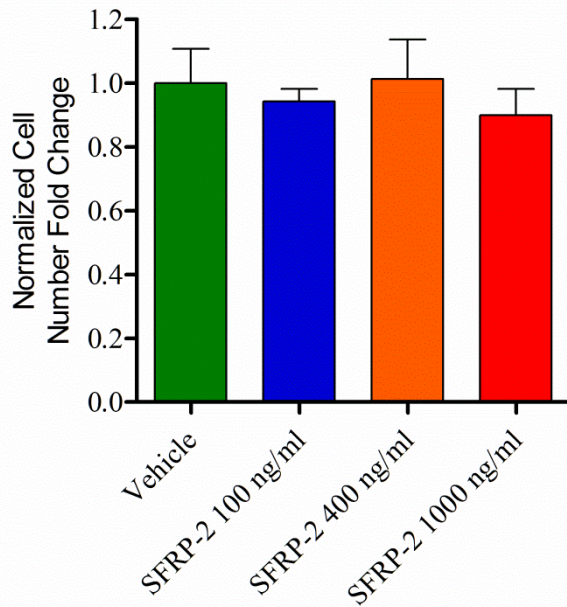
	1	2	3	4	5	6	7	8	9	10	11	12
A	Aes	Apc	Axin1	Bcl9	Btrc	Ctnnb1 p1	Ccnd1	Ccnd2	Ccnd3	Csnk1a1	Csnk1d	Csnk2a1
B	Ctbp1	Ctbp2	Ctnnb1	Daam1	Dixdc1	Dkk1	Dvl1	Dvl2	Ep300	Fbxw11	Fbxw2	Fbxw4
C	Fgf4	Fosl1	Foxn1	Frat1	Frzb	Fshb	Fzd1	Fzd2	Fzd3	Fzd4	Fzd5	Fzd6
D	Fzd7	Fzd8	Gsk3b	Jun	Kremen1	Lef1	Lrp5	Lrp6	Myc	Nkd1	NIK	Pitx2
E	Porcn	Ppp2ca	Ppp2r1a	Ppp2r5d	Pygo1	Rhou	Senp2	Sfrp1	Sfrp2	Sfrp4	Slc9a3r1	Sox17
F	T	Tcf7l1	Tcf7	Tle1	Tle2	Wif1	Wisp1	Wnt1	Wnt10a	Wnt11	Wnt16	Wnt2
G	Wnt2b	Wnt3	Wnt3a	Wnt4	Wnt5a	Wnt5b	Wnt6	Wnt7a	Wnt7b	Wnt8a	Wnt8b	Wnt9a
H	Gusb	Hprt	Hsp90ab1	Gapdh	Actb	MGDC	RTC	RTC	RTC	PPC	PPC	PPC

## Supplemental References

1. Mouquet F, Pfister O, Jain M, Oikonomopoulos A, Ngoy S, Summer R, Fine A, Liao R. Restoration of cardiac progenitor cells after myocardial infarction by self-proliferation and selective homing of bone marrow-derived stem cells. *Circ Res*. 2005;97(11):1090-1092.
2. Pfister O, Oikonomopoulos A, Sereti KI, Liao R. Isolation of resident cardiac progenitor cells by Hoechst 33342 staining. *Methods Mol Biol*. 2010;660:53-63.
3. Biechele TL, Moon RT. Assaying beta-catenin/TCF transcription with beta-catenin/TCF transcription-based reporter constructs. *Methods Mol Biol*. 2008;468:99-110.
4. Pfister O, Oikonomopoulos A, Sereti KI, Sohn RL, Cullen D, Fine GC, Mouquet F, Westerman K, Liao R. Role of the ATP-binding cassette transporter Abcg2 in the phenotype and function of cardiac side population cells. *Circ Res*. 2008;103(8):825-835.
5. Shi J, Guan J, Jiang B, Brenner DA, Del Monte F, Ward JE, Connors LH, Sawyer DB, Semigran MJ, Macgillivray TE, Seldin DC, Falk R, Liao R. Amyloidogenic light chains induce cardiomyocyte contractile dysfunction and apoptosis via a non-canonical p38alpha MAPK pathway. *Proc Natl Acad Sci U S A*. 2010;107(9):4188-4193.



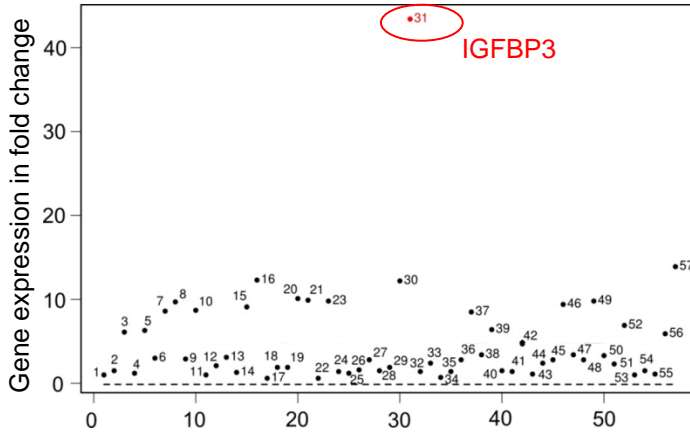
# Online Figure I



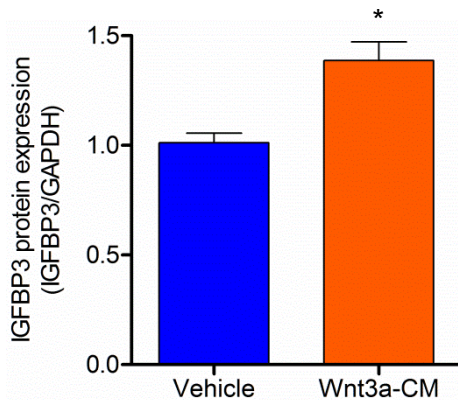
**Online Figure I: Administration of SFRP2 does not alter CSP cell proliferation capacity in vitro.** Treatment of CSP cells with increasing concentrations of SFRP2 protein had no effect on CSP cell numbers compared to Vehicle treated cells (n=3). Data are mean  $\pm$  s.e.m. Cell number in fold change is normalized to Vehicle group.

# Online Figure II

**A**

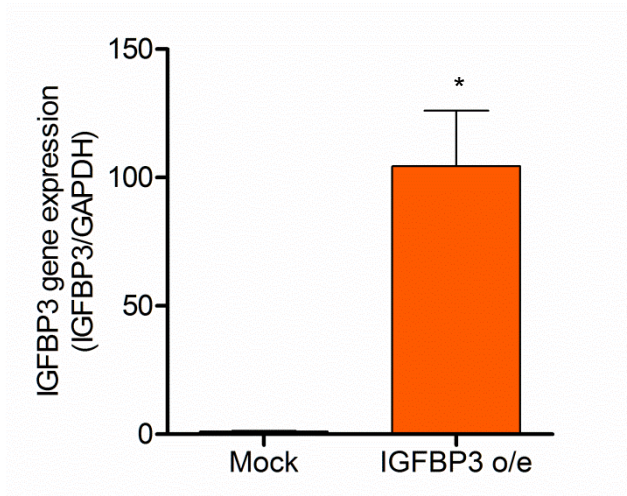


**B**



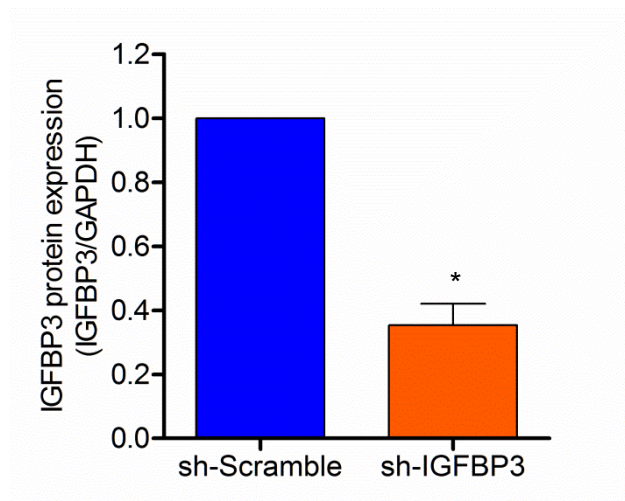
**Online Figure II: Activation of Wnt signaling pathway up-regulates IGFBP3 expression in CSP cells. (A)** Scatter plot analysis of pathway finder RT-PCR gene array in CSP cells following treatment (6 days) with Vehicle or Wnt3a-CM. IGFBP3 (red dot) was profoundly up-regulated among various genes related to different signaling pathways (n=3). The gene corresponding to each number can be found in Online Table II (second column). **(B)** Quantification of Western blot analysis of IGFBP3 protein expression in CSP cells following treatment with Wnt3a-CM (48 hours) (n=3). Data are mean  $\pm$  s.e.m. \*  $P \leq 0.05$ .

## Online Figure III



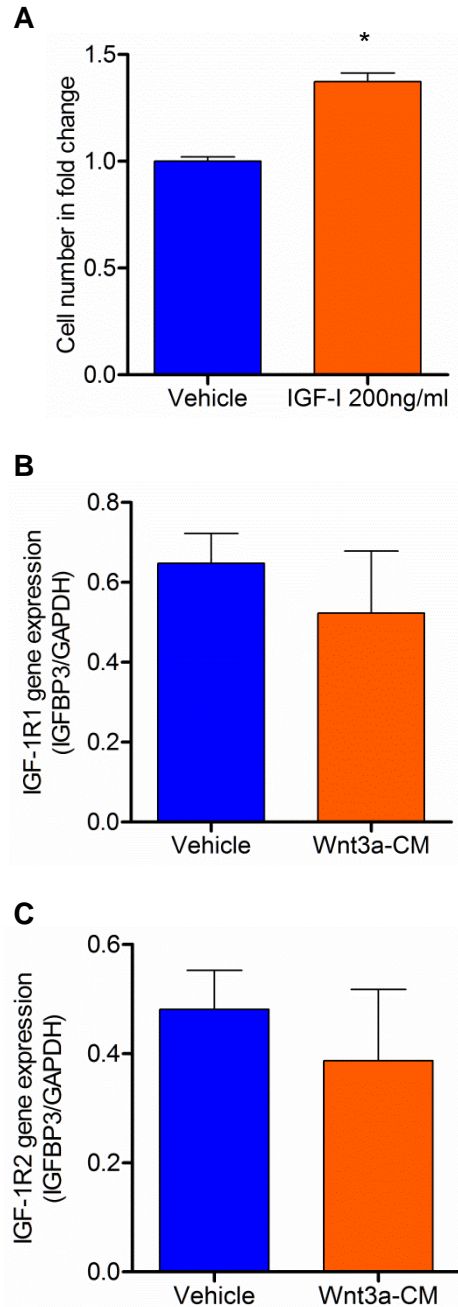
**Online Figure III: Lentivirus-mediated over-expression of IGFBP3.** RT-PCR mRNA expression analysis of IGFBP3 in CSP cells infected with Mock or IGFBP3-over-expressing lentivirus (IGFBP3 o/e) (n=3). Data are mean  $\pm$  s.e.m. \*  $P \leq 0.05$ .

## Online Figure IV



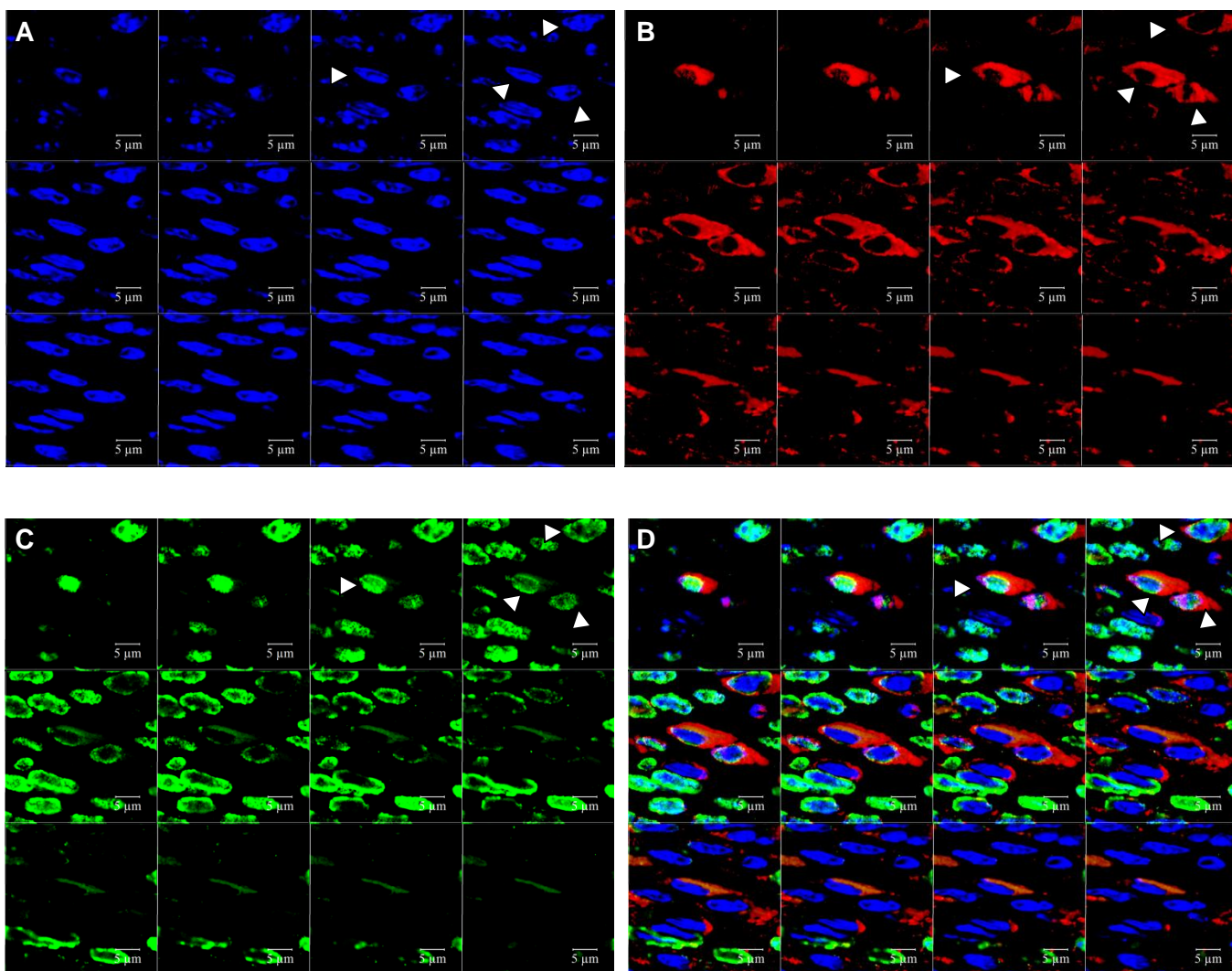
**Online Figure IV: shRNA mediated down-regulation of IGFBP3.** Quantification of Western blot analysis of IGFBP3 protein expression in sh-Scramble and sh-IGFBP3 CSP cells (n=3). Data are mean  $\pm$  s.e.m. \*  $P \leq 0.05$ .

# Online Figure V



**Online Figure V: IGF-1 increases CSP proliferation capacity.** (A) Treatment of CSP cells with 200ng/ml of IGF-1 protein resulted in increased proliferation capacity compared to Vehicle treated cells (n=3). RT-PCR mRNA expression analysis of (B) IGF-1R1 and (C) IGF-1R2 following Vehicle and Wnt3a treatment (n=3). Data are mean  $\pm$  s.e.m. \*  $P \leq 0.05$ . 33

# Online Figure VI



Alexa488 (BrdU)

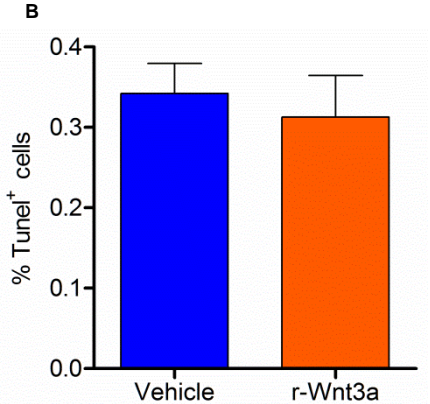
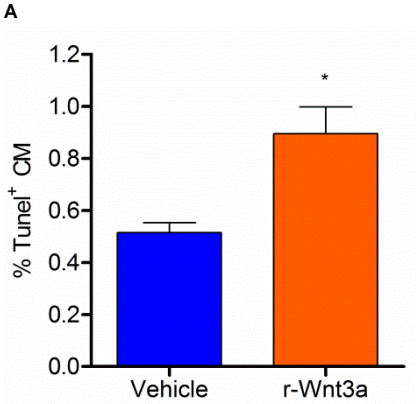
Alexa-555 ( $\alpha$ -s-Actin)

DAPI (Nuclei)

**Online Figure VI: BrdU<sup>+</sup> cardiomyocytes in infarct/border zone area of r-Wnt3a-injected heart.** (A-D) Each panel shows a series of 12 representative confocal z-stack immuno-fluorescent images of BrdU<sup>+</sup> cardiomyocytes in high magnification (x200). White arrowheads indicate the position of four BrdU<sup>+</sup> cardiomyocytes. Myocardial sections were immuno-labeled with (A) DAPI (blue), (B)  $\alpha$ -sarcomeric-actin (red), (C) BrdU (green). (D) Merged picture. (Scale bars, 5  $\mu$ m).

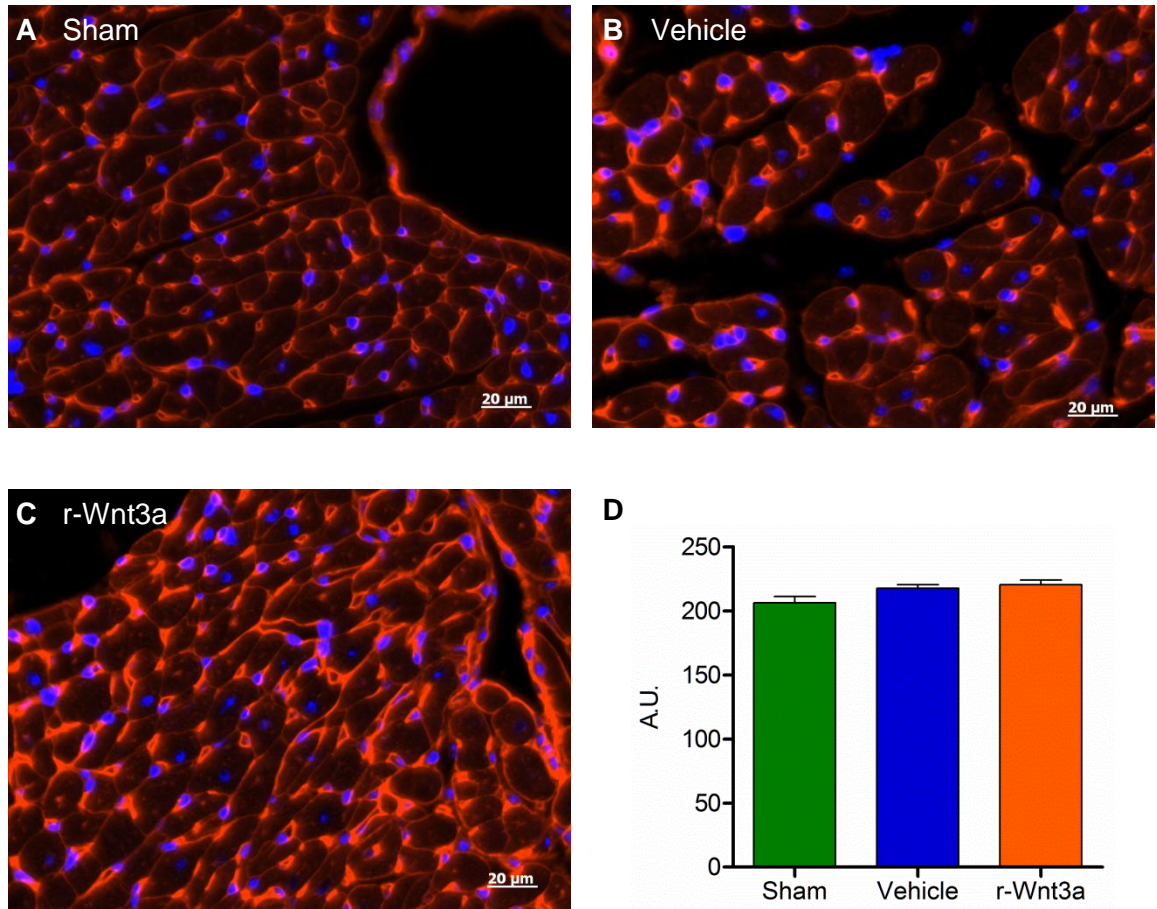


# Online Figure VII



**Online Figure VII: Administration of r-Wnt3a increases cardiomyocyte cell death post-MI.** Injection of r-Wnt3a resulted in **(A)** increased TUNEL<sup>+</sup> cardiomyocytes in the infarct/border zone area one week post-MI compared to Vehicle injected hearts. **(B)** r-Wnt3a had no effect on total cell death (Vehicle n=4, r-Wnt3a n=5).

# Online Figure VIII



**Online Figure VIII: Administration of r-Wnt3a does not alter cardiomyocyte cross-sectional area post-MI.** Representative examples of WGA staining in (A) Sham, (B) Vehicle and (C) r-Wnt3a injected hearts one week post-MI. (D) Quantification of cardiomyocyte cross-sectional area revealed no significant differences between the groups (n=4). Sections were immuno-labeled with WGA (red) and DAPI (blue). A.U. arbitrary units. (Scale bars 20 µm).